Published May 2, 2011

Occludin S408 phosphorylation regulates tight junction protein interactions and barrier function

David R. Raleigh,[1] Devin M. Boe,[1] Dan Yu,[1] Christopher R. Weber,[1] Amanda M. Marchiando,[1] Emily M. Bradford,[1] Yingmin Wang,[1] Licheng Wu,[1] Eveline E. Schneeberger,[3] Le Shen,[1,2] Jerrold R. Turner[1]

[1]Department of Pathology and [2]Department of Surgery, The University of Chicago, Chicago, IL 60637
[3]Molecular Pathology Unit, Massachusetts General Hospital, Charlestown, MA 02114

Although the C-terminal cytoplasmic tail of the tight junction protein occludin is heavily phosphorylated, the functional impact of most individual sites is undefined. Here, we show that inhibition of CK2-mediated occludin S408 phosphorylation elevates transepithelial resistance by reducing paracellular cation flux. This regulation requires occludin, claudin-1, claudin-2, and ZO-1. S408 dephosphorylation reduces occludin exchange, but increases exchange of ZO-1, claudin-1, and claudin-2, thereby causing the mobile fractions of these proteins to converge. Claudin-4 exchange is not affected. ZO-1 domains that mediate interactions with occludin and claudins are required for increases in claudin-2 exchange, suggesting assembly of a phosphorylation-sensitive protein complex. Consistent with this, binding of claudin-1 and claudin-2, but not claudin-4, to S408A occludin tail is increased relative to S408D. Finally, CK2 inhibition reversed IL-13–induced, claudin-2–dependent barrier loss. Thus, occludin S408 dephosphorylation regulates paracellular permeability by remodeling tight junction protein dynamic behavior and intermolecular interactions between occludin, ZO-1, and select claudins, and may have therapeutic potential in inflammation-associated barrier dysfunction.

Introduction

The tight junction (TJ) is a complex of transmembrane and peripheral membrane proteins that define the paracellular barrier (Mitic and Anderson, 1998; Tsukita and Furuse, 2002; Anderson and Van Itallie, 2009). Although binding of claudins to ZO-1 or ZO-2 is critical for TJ assembly (McNeil et al., 2006; Shin and Margolis, 2006; Umeda et al., 2006), the contributions of these and other interprotein interactions to barrier regulation in living cells are poorly understood. Recent analyses using FRAP and related techniques have demonstrated that, despite numerous physical links between TJ proteins, the molecular structure of the steady-state TJ is highly dynamic and TJ protein complexes undergo continuous remodeling with unique kinetics and varied mechanisms for each of the TJ complex components (Shen et al., 2008). We therefore hypothesized that modification of interactions between TJ proteins and resulting alterations in protein complex composition and stability might be a mechanism of barrier regulation.

ZO-1 is thought to primarily regulate paracellular permeability to uncharged macromolecules (Van Itallie et al., 2009a) via the leak pathway of trans-TJ flux (Anderson and Van Itallie, 2009; Turner, 2009; Weber et al., 2010). In contrast, conductance across the size- and charge-selective TJ paracellular pore pathway appears to be regulated by claudin proteins (Simon et al., 1999; Tsukita and Furuse, 2000; Van Itallie et al., 2008b; Anderson and Van Itallie, 2009; Rosenthal et al., 2010). The charge selectivity of these pores is determined by specific residues within the first extracellular loop of claudins (Balda et al., 2000; Furuse et al., 2001; Amasheh et al., 2002; Colegio et al., 2002, 2003; Van Itallie et al., 2003). For instance, paracellular pores created by claudin-2 allow small cations and water to pass, but exclude anions and larger solutes (Amasheh et al., 2002; Van Itallie et al., 2008b;

D.M. Boe, D. Yu, and C.R. Weber contributed equally to this paper.

Correspondence to Jerrold R. Turner: jturner@bsd.uchicago.edu; or Le Shen: leshen@uchicago.edu

Abbreviations used in this paper: DMAT, 2-dimethylamino-4,5,6,7-tetrabromo-1H-benzimidazole; EGFP, enhanced green fluorescent protein; FITC, fluorescein isothiocyanate; KD, knockdown; mRFP1, monomeric red fluorescent protein 1; TAMP, TJ-associated MARVEL protein; TBCA, tetrabromocinnamic acid; TER, transepithelial electrical resistance; TJ, tight junction.

Supplemental Material can be found at:
http://jcb.rupress.org/content/suppl/2011/04/29/jcb.201010065.DC1.html
Original image data can be found at:
http://jcb-dataviewer.rupress.org/jcb/browse/3452

The Rockefeller University Press $30.00
J. Cell Biol. Vol. 193 No. 3 565–582
www.jcb.org/cgi/doi/10.1083/jcb.201010065

Published May 2, 2011

Yu et al., 2009; Muto et al., 2010; Rosenthal et al., 2010). These pores appear to primarily be regulated by claudin-2 protein expression and half-life (Van Itallie et al., 2004; Heller et al., 2005; Weber et al., 2010) and, perhaps, by competition with other claudin family members (Van Itallie et al., 2001; Angelow et al., 2007). Although mathematical models of TJ barrier properties suggest that intra-TJ pores have defined open probabilities (Claude and Goodenough, 1973; Claude, 1978), neither the value nor regulation of this biophysical parameter has been determined.

The role of occludin in paracellular barrier function remains controversial (Saitou et al., 2000; Schulzke et al., 2005; Yu et al., 2005; Marchiando et al., 2010; Van Itallie et al., 2010), but hyperphosphorylation of the C-terminal cytoplasmic tail is associated with localization at TJs (Sakakibara et al., 1997; Wong, 1997). Several studies have assessed specific phosphorylated residues within occludin, and the region proximal to the C-terminal coiled-coil occludin/ELL (OCEL) domain appears to be a hotspot for functionally relevant sites. For example, T403 and T404 phosphorylation enhance both occludin trafficking to the TJ and paracellular barrier function (Suzuki et al., 2009). In contrast, phosphorylation of Y398 and Y402 reduces occludin–ZO-1 interactions, interferes with occludin localization at the TJ, and sensitizes monolayers to oxidant-induced barrier disruption (Elias et al., 2009). Similarly, phosphorylation of the more distal S490, which is located within the OCEL domain, attenuates the interaction between occludin and ZO-1 (Sundstrom et al., 2009) and is associated with occludin endocytosis and barrier loss (Murakami et al., 2009). Thus, although hyperphosphorylation is associated with occludin trafficking to the TJ, the impact of phosphorylation at specific sites within the C-terminal cytoplasmic tail is highly variable and may, at least in part, reflect modulation of ZO-1 binding.

The kinase CK2 (Litchfield et al., 2001; Meggio and Pinna, 2003) is known to phosphorylate occludin S408, T404, and, to a lesser extent, T400 in vitro and in vivo (Cordenonsi et al., 1999; Smales et al., 2003; Dörfel et al., 2009). Although the functional significance of CK2-mediated occludin phosphorylation has not been explored, S408 phosphorylation facilitates subsequent CK2-mediated phosphorylation at T404 and T400. This suggests that S408 phosphorylation is the rate-limiting step in CK2-mediated occludin phosphorylation (Dörfel et al., 2009). We therefore sought to determine the molecular and functional consequences of S408 occludin phosphorylation. The data indicate that S408 dephosphorylation reduces paracellular cation flux by stabilizing occludin–ZO-1 interactions that, in a ZO-1–dependent manner, enhance claudin-1 and claudin-2, but not claudin-4, exchange and prevent pore assembly or opening. Conversely, S408 phosphorylation enhances homotypic occludin–occludin interactions, releases ZO-1, and promotes paracellular cation flux via claudin-1– and claudin-2–based pores. We conclude that occludin S408 is a molecular switch by which CK2, and, potentially other occludin kinases, regulate TJ molecular remodeling, protein interactions, and paracellular pore function.

Results

CK2 decreases epithelial barrier function by amplifying paracellular ion flux

To determine if CK2 can regulate epithelial barrier function, polarized Caco-2 human intestinal epithelial cells were treated with the CK2 inhibitors 4,5,6,7-tetrabromobenzotriazole (TBB; IC_{50} 1 µM; Sarno et al., 2001), 2-dimethylamino-4,5,6,7-tetrabromo-1H-benzimidazole (DMAT; IC_{50} 0.15 µM; Pagano et al., 2004), and tetrabromocinnamic acid (TBCA; IC_{50} 0.11 µM; Pagano et al., 2007). Each significantly elevated transepithelial electrical resistance (TER) in a dose-dependent manner that correlated with drug potency (Fig. 1 A). Peak TER increases were achieved within 3 h and were sustained for at least three additional hours of treatment (Fig. 1 B).

Although the prolonged interval over which CK2 inhibition raises TER could allow protein synthesis or degradation, expression of ZO-1, claudin-1, claudin-2, or claudin-4, and the TJ-associated MARVEL proteins (TAMPs) occludin, tricellulin, and marvelD3, was unaffected (Fig. S1 A). Expression of these proteins was also unaffected by siRNA-mediated CK2 knockdown (Fig. S1, A–C), which increased TER to an extent comparable to enzymatic inhibition. Moreover, CK2 knockdown abrogated the ability of CK2 inhibitors to elevate TER (Fig. 1 C). Thus, the observed TER regulation is a function of CK2 inhibition, rather than off-target drug effects. Moreover, although previous studies have shown that CK2 can stimulate Na^+/H^+ exchanger 3 (NHE3; Sarker et al., 2008), which in turn can regulate TER (Turner et al., 2000), the effects of CK2 and NHE3 inhibition were additive (Fig. S1 D). Thus, the effect of CK2 inhibition on barrier function is independent of NHE3.

The 22 ± 1% increase in TER induced by 50 µM TBCA was accompanied by a 20 ± 1% decrease in paracellular Na^+ flux, but TJ permeability to cations with radii larger than ∼2.5 Å (Fig. 1 D), anions (not depicted), and uncharged macromolecules (Fig. S1 E) was unaffected. Therefore, CK2 regulates paracellular permeability of small cations through the pore pathway but does not affect leak pathway flux (Anderson and Van Itallie, 2009; Van Itallie et al., 2009b; Yu et al., 2009; Weber et al., 2010; Shen et al., 2011).

CK2-mediated barrier regulation is occludin dependent

Barrier regulation is commonly associated with TJ protein redistribution. Localizations of ZO-1, claudin-1, claudin-2, claudin-4, marvelD3, tricellulin, and occludin were therefore evaluated before and after CK2 inhibition. Only occludin distribution was affected (Fig. 2 A). CK2 inhibition increased TJ-associated occludin and decreased the number of occludin-containing cytoplasmic vesicles (Fig. 2, B and C). In contrast, CK2, which localizes to the cytoplasm, lateral membrane, and TJ of Caco-2 cells, was not redistributed after enzymatic inhibition (Fig. S1 F). Thus, barrier function increases after CK2 inhibition are associated with occludin redistribution to the TJ. Conversely, occludin removal from the TJ promotes barrier loss (Clayburgh et al., 2005; Shen and Turner, 2005; Murakami et al., 2009; Marchiando et al., 2010; Van Itallie et al., 2010). This suggests that TER

Published May 2, 2011

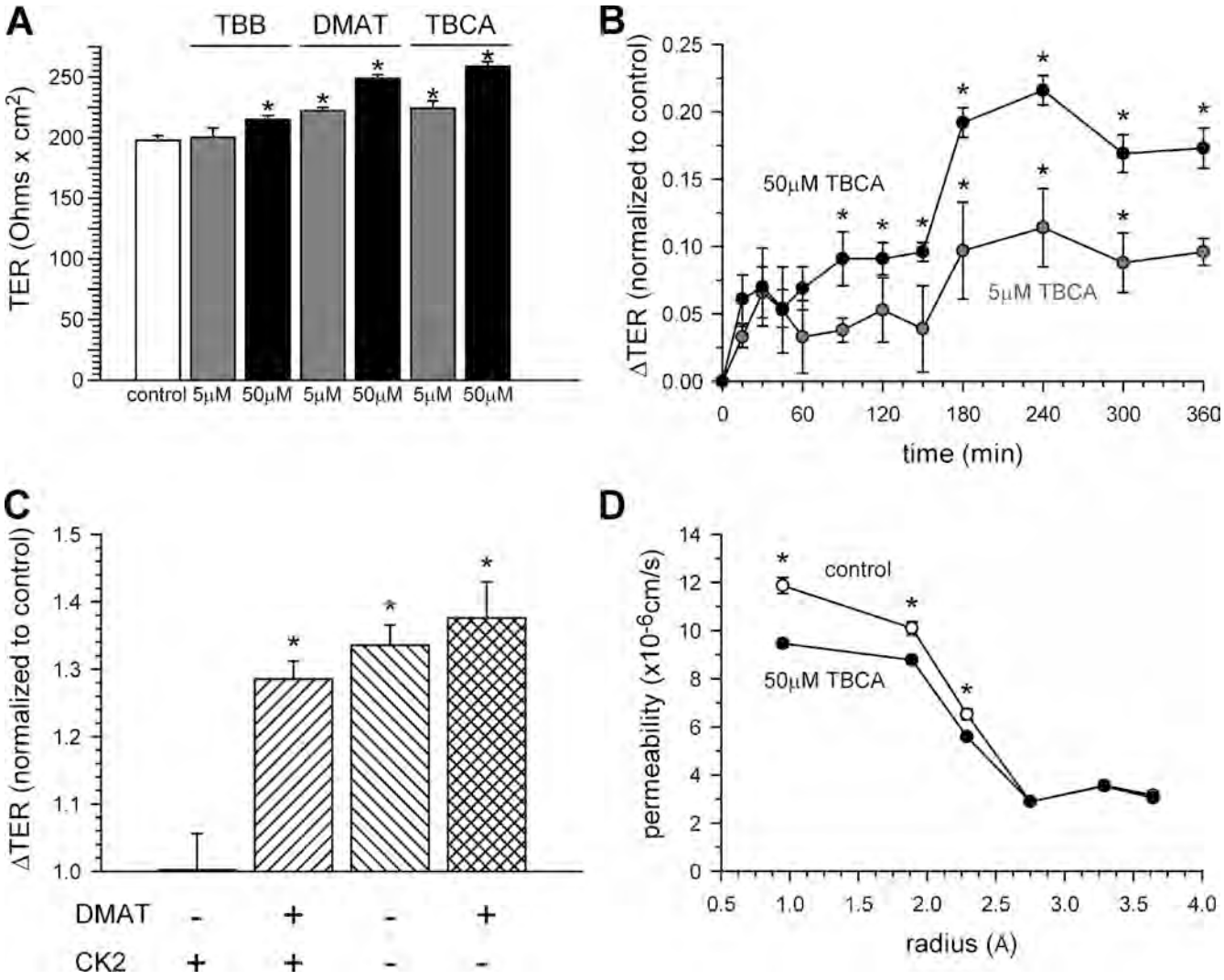

Figure 1. **CK2 decreases epithelial barrier function by amplifying paracellular ion flux.** (A) CK2 inhibitors elevated Caco-2 TER in a dose-dependent manner after 5 h of treatment. (B) CK2 inhibition caused maximal TER increases within 3 h. (C) Chemical inhibition or CK2 knockdown resulted in comparable TER increases after 6 h of DMAT (50 μM) treatment. (D) Biionic potentials of sodium, methylamine, ethylamine, tetramethylammonium, tetraethylammonium, and *N*-methyl-D-glucamine were measured 4 h after TBCA (50 μM) addition.

regulation by CK2 may require occludin. To assess this, Caco-2 cells in which occludin expression was stably knocked down were developed. Occludin knockdown monolayers did not increase TER regulation after CK2 inhibition (Fig. 2 D), indicating an essential role of occludin in this form of barrier regulation. However, NHE3 inhibition increased TER of monolayers lacking occludin (Fig. S1 G), demonstrating that occludin knockdown monolayers are capable of barrier regulation and providing further evidence that the observed effects of CK2 inhibition are not related to NHE3. Thus, CK2 regulates TJ barrier function in an occludin-dependent manner.

CK2 inhibition stabilizes occludin, but not other TAMPs, at the TJ

To determine if CK2-dependent barrier regulation is associated with alterations in TJ protein dynamic behavior, FRAP was used to assess exchange of occludin and the related TAMPs tricellulin, marvelD3 variant 1, and marvelD3 variant 2 (Raleigh et al., 2010). The occludin mobile fraction was reduced from 71 ± 4% to 50 ± 4% ($P < 0.01$) after CK2 inhibition (Fig. 3, A and B). In contrast, mobile fractions of tricellulin or either marvelD3 splice variant were unaffected (Fig. 3, A and B). CK2 knockdown both reduced the occludin mobile fraction and rendered occludin recovery resistant to pharmacological CK2 inhibition (Fig. 3 C; Fig. S2 A; Table I). Thus, CK2 inhibition increases both the quantity and stability of TJ-associated occludin while increasing barrier function. Together, these data suggest that occludin recruitment and stabilization may be involved in the observed barrier regulation.

CK2 inhibition stabilizes occludin at the TJ in vivo

To determine if the effect of CK2 inhibition on occludin dynamic behavior in cell culture is an accurate recapitulation of in vivo biology, FRAP was performed using transgenic mice expressing EGFP-occludin under control of the villin promoter

Published May 2, 2011

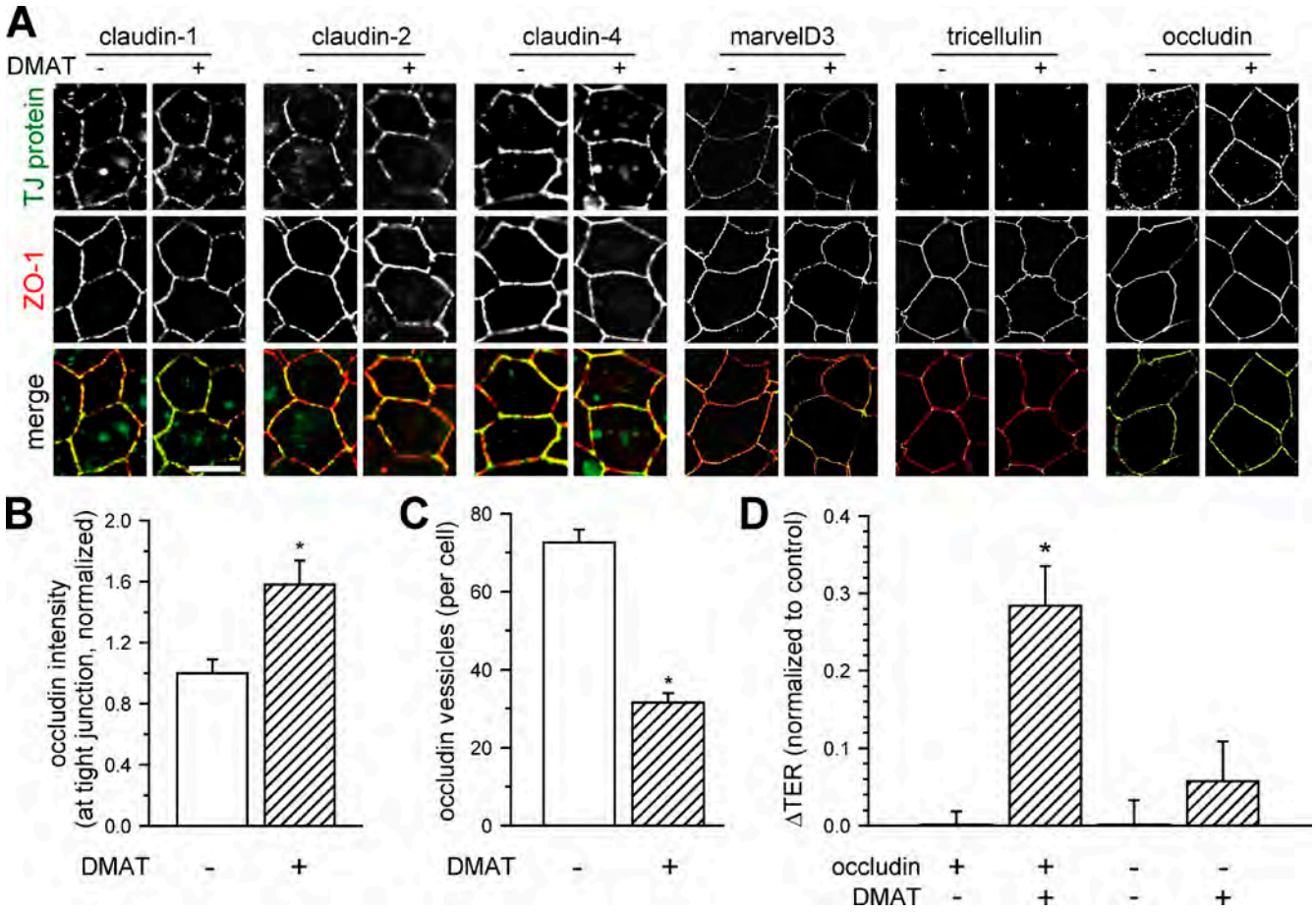

Figure 2. **CK2-mediated barrier regulation is occludin dependent.** (A) Effect of CK2 inhibition (50 µM DMAT) on distribution of transmembrane TJ proteins (green) and ZO-1 (red). Bar, 10 µm. (B) Quantitative analysis of occludin enrichment at the TJ. (C) Quantitative analysis of number of occludin-containing vesicles. (D) CK2 inhibition (50 µM DMAT) failed to elevate TER of occludin knockdown monolayers.

(Marchiando et al., 2010). CK2 inhibition significantly decreased the mobile fraction of occludin, from 57 ± 2% to 39 ± 1%, in vivo ($P < 0.01$) without altering the $t_{1/2}$ of recovery or TJ protein expression (Fig. 3 D; Fig. S2, B–D). Thus, CK2 inhibition stabilizes occludin at the TJ in vivo in a manner similar to that observed in vitro. Notably, the failure of CK2 inhibition to affect paracellular flux of water or BSA in vivo (Fig. S2 E) is consistent with the in vitro data showing that CK2 affects size-selective barrier regulation and that NHE3 is not involved in this process.

Phosphorylation at S408 is required for CK2-mediated occludin regulation

To identify the residue(s) responsible for CK2 regulation of barrier function and occludin exchange, alanine (A) or aspartic acid (D) mutations were introduced at T404 and S408, the two primary sites of CK2-mediated occludin phosphorylation. EGFP-occludin mutants were expressed in occludin knockdown Caco-2 cells to avoid potential interactions with endogenous wild-type occludin and were efficiently trafficked to TJs. Similar to endogenous occludin, wild-type EGFP-occludin was enriched at the TJ after CK2 inhibition (Fig. S3, A and B). The mobile fractions of T404D/S408D, T404A, and S408D mutants were indistinguishable from that of wild-type EGFP-occludin at baseline (68 ± 4%, 68 ± 8%, 69 ± 3%, and 70 ± 4%, respectively; Fig. 4, A and B). In contrast, the mobile fractions of EGFP-occludin T404A/S408A and S408A were significantly reduced (52 ± 3% and 49 ± 3%, respectively), and were similar to those of wild-type and T404A EGFP-occludin after CK2 inhibition (47 ± 2% and 45 ± 4%, respectively). Moreover, FRAP behavior of occludin T404D/S408D, T404A/S408A, S408A, and S408D mutants was unaffected by CK2 inhibition (Fig. 4, A and B; Table I). Thus, S408, but not T404, is critical to occludin exchange at the TJ. S408 is also the key regulator of occludin trafficking, as EGFP-occludin S408A was enriched at the TJ relative to wild-type or S408D EGFP-occludin and neither S408A nor S408D mutants were redistributed after CK2 inhibition (Fig. S3, A and B).

Occludin phosphorylation at S408 is required for CK2-mediated barrier regulation

The effect of S408 mutations on FRAP behavior and TJ localization suggests that this residue may also be essential for CK2-mediated barrier regulation. To test this hypothesis, we measured the effect of CK2 inhibition on TER of wild-type or occludin knockdown Caco-2 monolayers as well as on TER of knockdown cell lines stably expressing wild-type or mutant EGFP-occludin. Neither occludin knockdown nor expression of

Published May 2, 2011

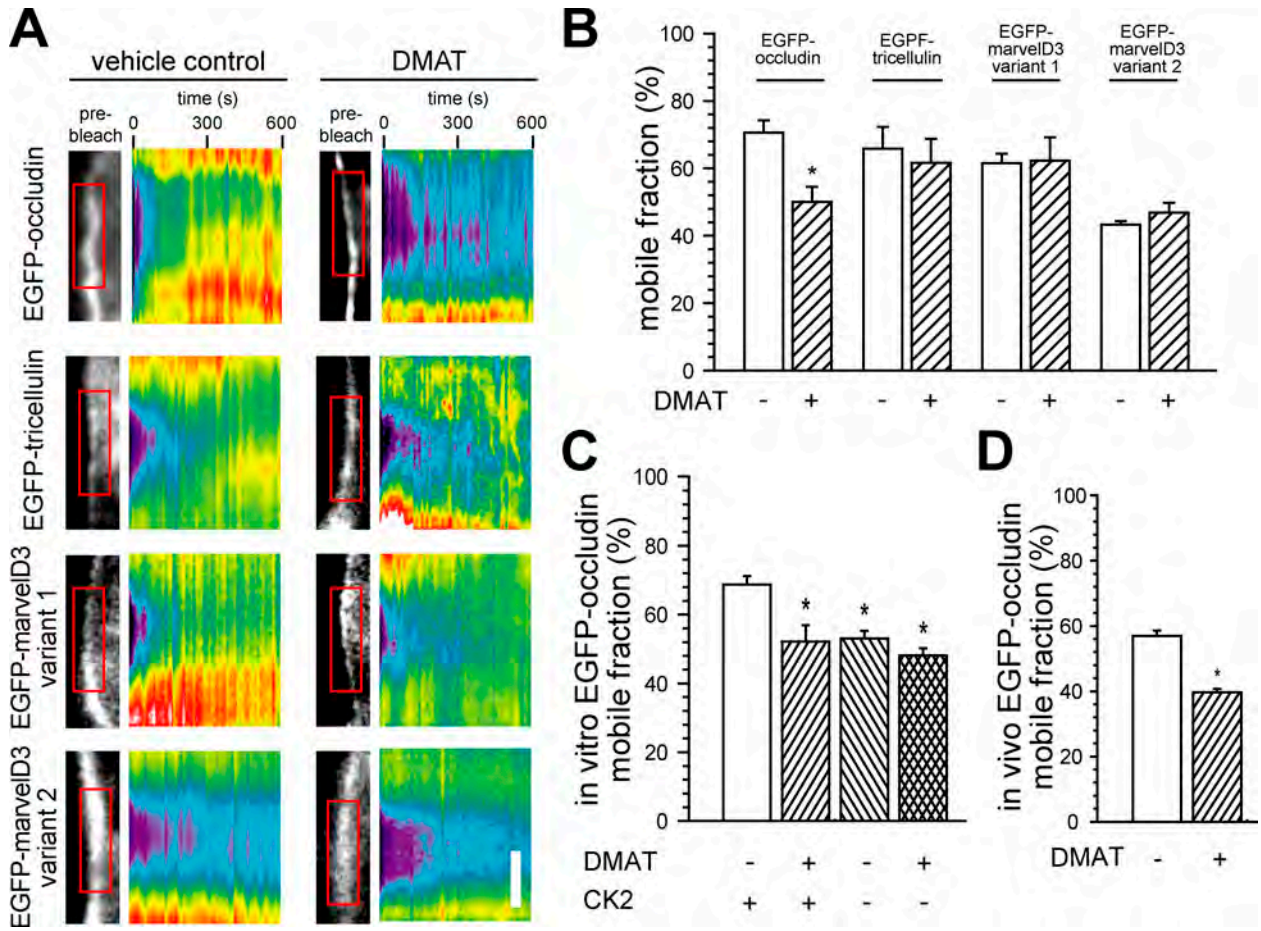

Figure 3. **CK2 inhibition stabilizes occludin at the TJ in vitro and in vivo.** (A) Kymographs of EGFP-TAMP FRAP, with or with out DMAT treatment (50 µM) at bicellular TJ regions. Bar, 3 µm. (B) Effect of CK2 inhibition (50 µM DMAT) on EGFP-TAMP mobile fractions. (C) EGFP-occludin mobile fraction after CK2 knockdown or chemical CK2 inhibition (50 µM DMAT). (D) Effect of CK2 inhibition (50 µM DMAT) on EGFP-occludin FRAP in mouse jejunum in vivo.

EGFP-occludin constructs altered expression of endogenous TJ proteins or CK2 (Fig. S3 C). However, occludin knockdown did reduce steady-state TER (Fig. S3 D). Expression of EGFP-tagged wild-type and T404A occludin, but not EGFP alone, restored TER responses to CK2 inhibition (Fig. 4 C). In contrast, neither T404D/S408D nor S408A EGFP-occludin–expressing monolayers were sensitive to CK2 inhibition. Therefore, both occludin expression and phosphorylation at S408 are necessary for CK2-mediated barrier regulation. Moreover, the parallel roles of S408 in occludin trafficking and exchange as well as barrier regulation suggests that these processes are linked.

Occludin S408 dephosphorylation enhances interactions with claudin-1, claudin-2, and ZO-1

S408 is located within a structurally disordered region of the cytoplasmic C-terminal tail of human occludin (Li et al., 2005; Walter et al., 2009). This site is adjacent to C409, which is critical for occludin dimerization (Li et al., 2005; Walter et al., 2009), and suggests that that S408 phosphorylation may modify occludin association with other proteins. To explore this hypothesis, GST-fusion constructs of wild-type occludin 383–522 or mutants with either S408D or S408A substitutions were expressed as recombinant proteins and immobilized on glutathione-agarose. These were used to probe Caco-2 lysates, and captured proteins were analyzed by immunoblot. Consistent with a role for S408 in regulation of occludin dimerization, the S408D occludin tail captured 2.4 ± 0.05-fold more endogenous occludin than the S408A tail (Fig. 5 A; $P < 0.05$). In contrast, the S408A tail recovered claudin-1 and claudin-2 more efficiently, and captured 5.1 ± 1.3 ($P < 0.01$) and 2.8 ± 0.3-fold ($P < 0.01$) more of each, respectively, relative to the S408D tail. These differences were specific to claudin-1 and claudin-2, as similar amounts of marvelD3 and claudin-4 were captured by the three occludin tail constructs, and GST alone failed to recover any of these proteins (Fig. 5 A).

The occludin cytoplasmic tail has not been reported to interact directly with claudins. However, ZO-1 interacts with both occludin and claudins (Furuse et al., 1994; Itoh et al., 1999a; Nusrat et al., 2000; Schmidt et al., 2001). Thus, ZO-1 may serve as an intermediate in occludin–claudin-1/claudin-2 interactions that are regulated by S408 phosphorylation. To assess direct interactions between ZO-1 and occludin, binding of recombinant VSV G epitope-tagged ZO-1 U5-GuK domain (Kreis, 1986; Raleigh et al., 2010) to immobilized GST-occludin 383–522 S408D and S408A was assessed. Both GST-occludin tails, but

Published May 2, 2011

Table I. **The dynamic behavior of TJ components involved in CK2-mediated epithelial barrier regulation**

	Epithelium	Pharmacological CK2 inhibition	Mobile fraction (%)
Occludin	Wild type		68 ± 3†
	Wild type	√	52 ± 5ª
	CK2 knockdown		53 ± 2ª
	CK2 knockdown	√	48 ± 2ª
	ZO-1 knockdown		67 ± 8
	In vivo		57 ± 2†
	In vivo	√	39 ± 1ª
T404D/S408D	Occludin knockdown		68 ± 4
	Occludin knockdown	√	69 ± 6
T404A/S408A	Occludin knockdown		52 ± 3ª
	Occludin knockdown	√	50 ± 3ª
T404A	Occludin knockdown		68 ± 8
	Occludin knockdown	√	45 ± 4ª
S408A	Occludin knockdown		49 ± 3ª
	Occludin knockdown	√	48 ± 7ª
	ZO-1 knockdown		70 ± 1
S408D	Occludin knockdown		69 ± 3
	Occludin knockdown	√	72 ± 3
	ZO-1 knockdown		66 ± 9
Claudin-1	Occludin knockdown		36 ± 2
	Occludin knockdown/wild-type occludin expression		37 ± 1†
	Occludin knockdown/S408D occludin expression		35 ± 4
	Occludin knockdown/S408A occludin expression		57 ± 3ª
Claudin-2	Wild type		33 ± 3†
	Occludin knockdown		33 ± 3
	Occludin knockdown/wild-type occludin expression		31 ± 5
	Occludin knockdown/S408D occludin expression		25 ± 6
	Occludin knockdown/S408A occludin expression		51 ± 2ª
	Wild type	√	51 ± 5
	Occludin knockdown	√	27 ± 1
	ZO-1 knockdown	√	32 ± 2
	ZO-1 knockdown/ZO-1 expression		35 ± 6
	ZO-1 knockdown/ZO-1 expression	√	54 ± 4ª
	ZO-1 knockdown/ZO-1 ΔPDZ1 expression		35 ± 4
	ZO-1 knockdown/ZO-1 ΔPDZ1 expression	√	28 ± 4
	ZO-1 knockdown/ZO-1 ΔU5-Guk expression		33 ± 5
	ZO-1 knockdown/ZO-1 ΔU5-Guk expression	√	32 ± 3
ZO-1	Wild type		48 ± 3†
	Wild type	√	60 ± 4ª
	Occludin knockdown		46 ± 4
	Occludin knockdown	√	45 ± 4
	Occludin knockdown/wild-type occludin expression		45 ± 4
	Occludin knockdown/S408D occludin expression		43 ± 4
	Occludin knockdown/S408A occludin expression		61 ± 4ª
	Wild-type/large area FRAP (center)		51 ± 4
	Wild-type/large area FRAP (edge)		50 ± 5†
	Wild-type/large area FRAP (center)	√	46 ± 1
	Wild-type/large area FRAP (edge)	√	58 ± 4ª

ªData are significant ($P < 0.05$) relative to control conditions (†).

not GST alone, bound to ZO-1 U5-GuK (Fig. 5 B). However, binding to the S408A tail was 3.2 ± 0.3-fold greater than to the S408D mutant ($P < 0.01$). These results suggest that interactions between occludin and ZO-1 are weakened by S408 phosphorylation. Together with the enhanced capture of full-length, endogenous occludin by the S408D occludin tail, these data also

Published May 2, 2011

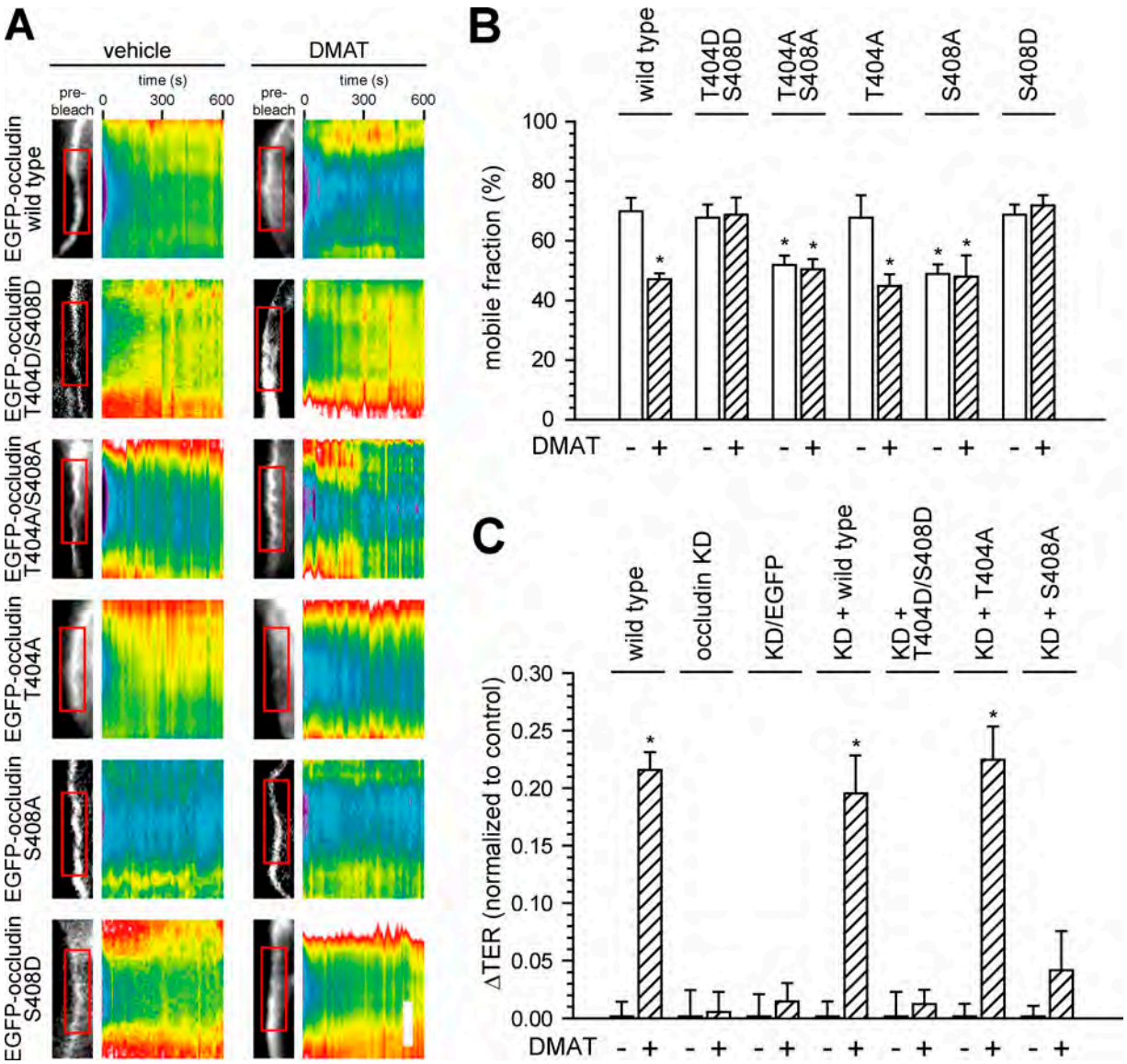

Figure 4. **S408 phosphorylation is required for CK2-mediated regulation of occludin dynamics and barrier function.** (A and B) FRAP analysis of EGFP-occludin mutants expressed in occludin knockdown Caco-2 cells. Bar, 3 µm. (C) Expression of EGFP or EGFP-occludin mutants in occludin knockdown (KD) Caco-2.

support the hypothesis that S408 phosphorylation acts as a molecular switch that determines whether occludin forms homodimers or heterotypic interactions with ZO-1.

The enhanced association of the ZO-1 U5-GuK construct with S408A occludin tail is consistent with a model where ZO-1 mediates interactions between occludin and claudin-1 or claudin-2. To determine if ZO-1 is required for claudin capture by immobilized GST-occludin 383–522, lysates of ZO-1 knockdown Caco-2 cells were probed with immobilized S408A and S408D occludin tails. ZO-1 knockdown almost completely eliminated claudin-2 recovery, and there was no difference between amounts captured by S408A and S408D occludin tails (Fig. 5 C). Thus, ZO-1 mediates S408 phosphorylation-regulated occludin interactions with claudin-2. Importantly, ZO-1 knockdown did not affect expression of ZO-2, or claudins 1, 2, or 4 (Fig. S4 A).

Occludin S408 dephosphorylation increases claudin-1, claudin-2, and ZO-1 exchange at the TJ

The studies above used cell lysates and recombinant proteins to show that S408 phosphorylation reduces interactions between occludin, ZO-1, claudin-1, and claudin-2. However, the large number of protein interactions at TJs may allow larger complexes to form within intact epithelial monolayers and make S408 phosphorylation irrelevant. Thus, as an indirect measure of protein interactions, mobile fractions were assessed by FRAP in confluent Caco-2 monolayers. Pharmacological CK2 inhibition in wild-type monolayers increased the mobile fraction of TJ-associated mRFP1-ZO-1 from 48 ± 3% to 60 ± 4% (Fig. 5 D; $P < 0.05$) but did not affect ZO-1 exchange in occludin knockdown monolayers. Moreover, S408A, but not wild-type or S408D EGFP-occludin increased mRFP1-ZO-1 exchange in a

Published May 2, 2011

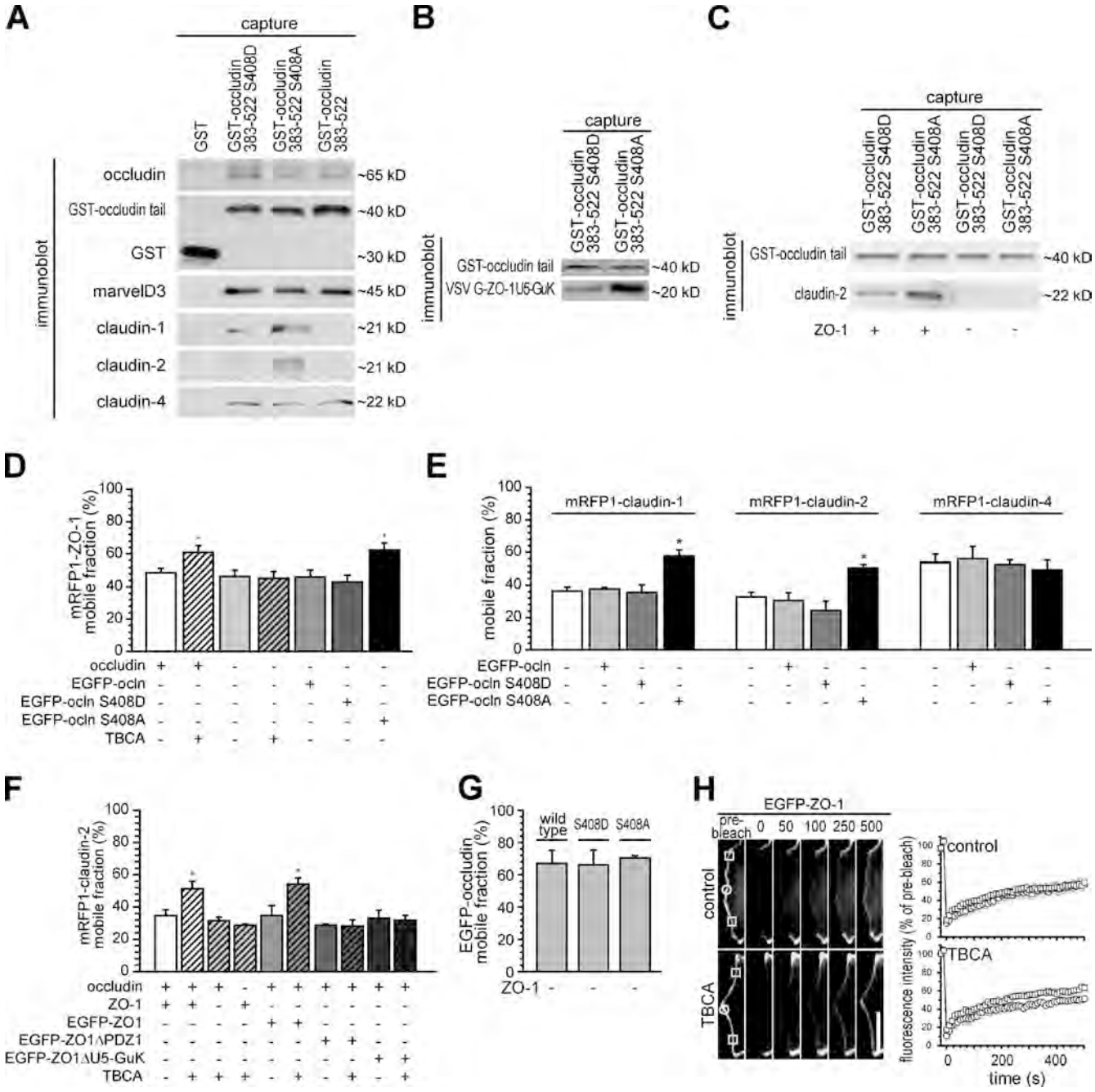

Figure 5. **Occludin S408 dephosphorylation enhances interactions with claudin-1, claudin-2, and ZO-1, and their exchange at the TJ.** (A) GST-occludin C-terminal tails (383–522) immobilized on glutathione-agarose were used to probe Caco-2 lysates, and recovered proteins assessed by SDS-PAGE immunoblot. (B) GST-occludin C-terminal tails were used to capture VSV G-ZO-1-U5-GuK. (C) GST-occludin C-terminal tails were used to probe control and ZO-1 knockdown Caco-2 lysates, as above. (D) FRAP of mRFP1-ZO-1 was assessed in control and occludin knockdown monolayers as well as occludin knockdown monolayers expressing wild-type, S408D, or S408A EGFP-occludin. (E) FRAP of mRFP1-tagged claudin-1, claudin-2, and claudin-4 were assessed in occludin knockdown monolayers either alone or with wild-type, S408D, or S408A EGFP-occludin. (F) FRAP analysis of mRFP1-claudin-2 expressed in wild-type, occludin knockdown, or ZO-1 knockdown monolayers as well as ZO-1 knockdown monolayers expressing wild-type, ΔPDZ1, or ΔU5-GuK EGFP-ZO-1. (G) FRAP of wild-type, S408D, and S408A EGFP-occludin in ZO-1 knockdown monolayers. (H) EGFP-ZO-1 fluorescent recovery at the center (circles) and edges (squares) of elongated bleach regions. Bar, 6 µm. Chemical CK2 inhibition throughout this figure was with 50 µM TBCA

manner similar to CK2 inhibition (Fig. 5 D; $P < 0.05$). Thus, occludin S408 dephosphorylation enhances ZO-1 exchange at the TJ.

Based on the in vitro binding studies, the effects of wild-type, S408D, and S408A EGFP-occludin expression on mRFP1-claudin exchange were assessed. S408A EGFP-occludin expression markedly increased the mobile fractions of both mRFP1–claudin-1 and claudin-2 (Fig. 5 E); CK2 inhibition had a similar effect on mRFP1–claudin-2 exchange (Fig. 5 F). In contrast, FRAP behavior of mRFP1–claudin-4 was comparable in occludin knockdown monolayers and those expressing wild-type, S408D, or S408A EGFP-occludin (Fig. 5 E). Thus, in a manner that parallels the protein binding assay data, occludin S408 dephosphorylation affects exchange of claudin-1 and claudin-2, but not claudin-4.

Published May 2, 2011

Table II. **CK2-mediated regulation of occludin, claudin-1, claudin-2, and ZO-1 mobile fractions**

Condition	Occludin	Claudin-1	Claudin-2	ZO-1
Steady state	68 ± 3	36 ± 2	33 ± 3	48 ± 3
CK2 inhibition	52 ± 5[a,b]		51 ± 5[a]	60 ± 4[a]
Occludin knockdown/occludin S408A	49 ± 3[a]	57 ± 3[a]	51 ± 2[a]	61 ± 4[a]
Occludin knockdown/CK2 inhibition			27 ± 1	45 ± 4
ZO-1 knockdown/CK2 inhibition			32 ± 2	

[a]Data changes are significant ($P < 0.05$) relative to steady state.

[b]Data were confirmed by in vitro CK2 knockdown and in vivo CK2 inhibition.

To determine whether the observed increase in claudin-2 exchange requires occludin or ZO-1, mRFP1–claudin-2 FRAP was assessed in wild-type, occludin knockdown, and ZO-1 knockdown monolayers. Although pharmacological CK2 inhibition increased mRFP1–claudin-2 exchange in wild-type monolayers, the mRFP1–claudin-2 mobile fraction was unchanged in occludin or ZO-1 knockdown monolayers (Fig. 5 F). Thus, similar to the binding assays, the FRAP studies indicate that ZO-1 is required for the effects of occludin S408 dephosphorylation on claudin-2 exchange.

The data support the hypothesis that ZO-1 acts as a scaffold that links occludin to claudin-2. The sites within ZO-1 that mediate binding to claudins (PDZ1) and occludin (U5-GuK) are well defined (Fanning et al., 1998, 2007; Itoh et al., 1999a; Schmidt et al., 2004; Li et al., 2005; Müller et al., 2005; Umeda et al., 2006). To assess the roles of these ZO-1 domains in regulation of claudin-2 exchange, ZO-1 knockdown Caco-2 cells were cotransfected with mRFP1–claudin-2 and either wild-type, ΔPDZ1, or ΔU5-GuK EGFP-ZO-1. Wild-type EGFP–ZO-1 restored sensitivity of mRFP1–claudin-2 recovery to CK2 inhibition. In contrast, EGFP–ZO-1 lacking either the PDZ1 or U5-GuK domain failed to restore sensitivity of mRFP1–claudin-2 recovery to CK2 inhibition (Fig. 5 F).

When taken together with the in vitro binding assays, the FRAP studies of confluent monolayers suggest that physical interactions among occludin, ZO-1, and select claudins are facilitated by occludin S408 dephosphorylation. Consistent with this, the markedly different occludin, ZO-1, and claudin-2 mobile fractions of 68 ± 3%, 48 ± 3%, and 33 ± 3%, respectively, converge to 52 ± 5%, 60 ± 4%, and 51 ± 5%, respectively, after CK2 inhibition (Table II). Moreover, (a) the mobile fraction of wild-type occludin after CK2 inhibition is similar to that of EGFP-occludin S408A; (b) FRAP behaviors of wild-type, S408D, and S408A EGFP-occludin are similar in ZO-1 knockdown cells (Fig. 5 G); and (c) S408A occludin expression increases ZO-1, claudin-1, and claudin-2 exchange in a manner similar to CK2 inhibition (Table II). These data are all consistent with the hypothesis that occludin S408 dephosphorylation promotes assembly of protein complexes that include occludin, ZO-1, claudin-1, and claudin-2.

Previous analyses have shown that fluorescent recovery of occludin and ZO-1 occur by diffusion within the plasma membrane and exchange with cytosolic pools, respectively (Shen et al., 2008). Thus, if occludin S408 dephosphorylation does promote complex assembly, the mechanism of ZO-1 recovery would be expected to change to include a component due to intramembrane diffusion. Although multiple approaches can be used, intramembrane diffusion and cytosolic exchange are most readily distinguished by analysis of FRAP over extended TJ regions (Shen et al., 2008). As reported previously in MDCK cells (Shen et al., 2008), EGFP–ZO-1 recovery in control Caco-2 cells was uniform over the bleached region, consistent with cytosolic exchange (Fig. 5 H). In contrast, EGFP–ZO-1 recovery at the periphery of bleached regions was significantly increased after CK2 inhibition (Table I; $P < 0.05$), whereas recovery at the center of bleached regions was unchanged (Fig. 5 H). Thus, the observed increases in ZO-1 mobile fraction are due to enhanced recovery at the edges in a pattern typical of intramembranous diffusion. These data support the hypothesis that S408 dephosphorylation enhances occludin association with ZO-1 in living cells.

CK2-mediated barrier regulation requires ZO-1, claudin-1, and claudin-2

Together with reports that claudin-2 creates a small cation-selective paracellular pore (Amasheh et al., 2002; Van Itallie et al., 2008b; Yu et al., 2009), the increased claudin-2 mobile fraction and decreased paracellular cation permeability induced by CK2 inhibition suggest that the S408 dephosphorylation may disrupt assembly or opening of claudin-2 pores. This would directly link occludin dynamic behavior to TJ barrier function and suggest that the effects of CK2 inhibition on cation-selective paracellular flux may require occludin, ZO-1, and claudin-2. Consistent with this, CK2 inhibition induced dose-dependent TER increases and Na^+ selectivity decreases in control, but not occludin knockdown, monolayers (Fig. 6, A and B). Thus, although occludin is not thought to form paracellular pores, it is required for regulation of paracellular Na^+ conductance and barrier function after CK2 inhibition. Similarly, ZO-1 knockdown eliminated TER and Na^+ selectivity responses to CK2 inhibition (Fig. 6, C and D). Thus, consistent with the in vitro binding and FRAP data, ZO-1 is also required for CK2-mediated regulation of paracellular cation pores.

Both biochemical and FRAP data suggest that roles of occludin and ZO-1 in CK2-mediated barrier regulation are, primarily, to control claudin-2 function. This is also consistent with the observation that CK2 inhibition regulates paracellular flux of small cations that are characteristic of claudin-2–based pores. To directly assess the participation of claudin-2 in CK2-mediated barrier regulation, stable claudin-2 knockdown Caco-2 cells were developed (Fig. S4 B). As expected, claudin-2 knockdown markedly increased TER (Fig. 6 E), reduced Na^+ selectivity

Published May 2, 2011

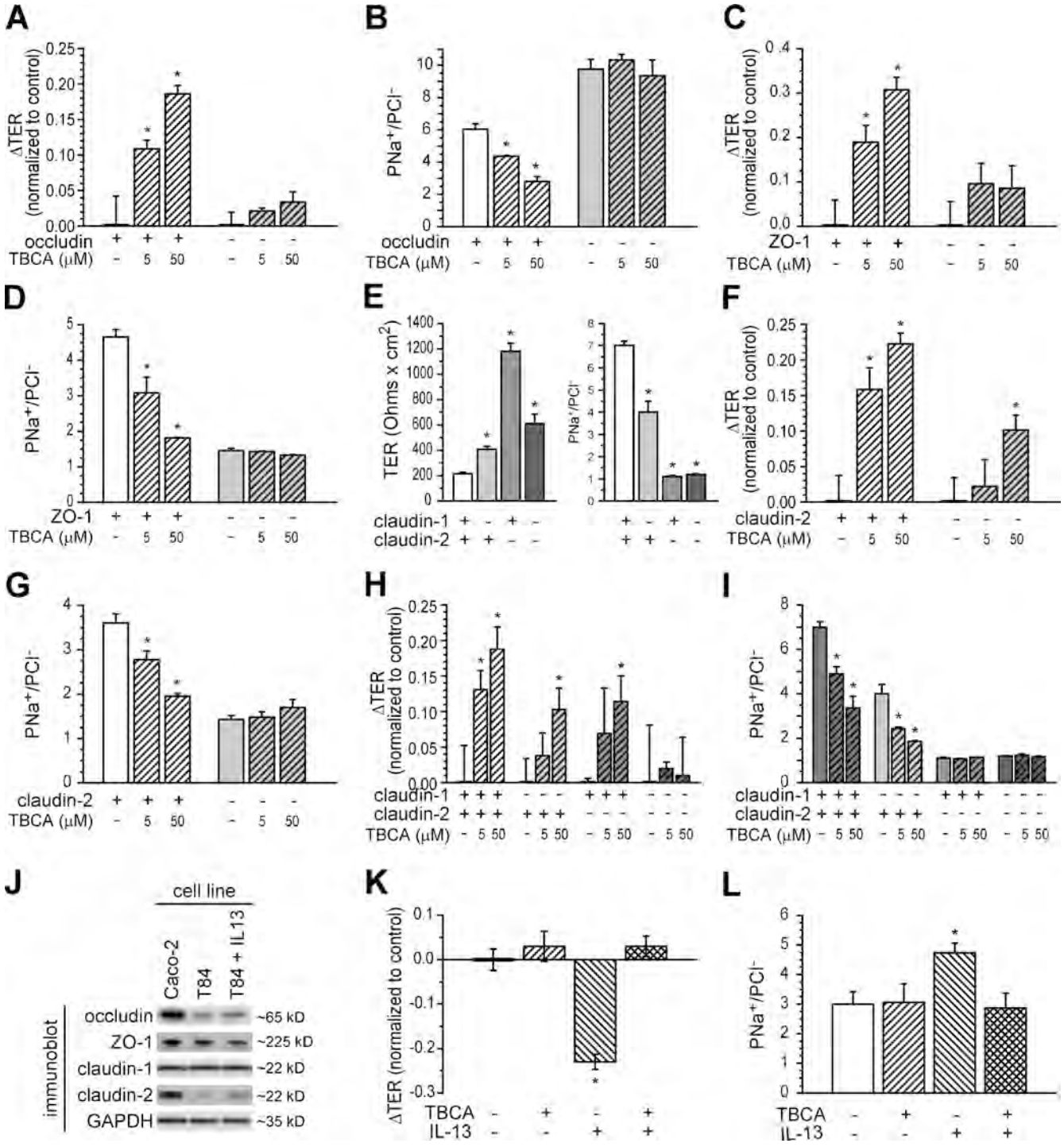

Figure 6. **CK2-mediated barrier regulation requires ZO-1 and claudin-2.** (A and B) TER and PNa^+/PCl^- responses of control and occludin knockdown monolayers to CK2 inhibition. (C and D) TER and PNa^+/PCl^- responses of control and ZO-1 knockdown monolayers to CK2 inhibition. (E) TER and PNa^+/PCl^- after claudin-1 and claudin-2 knockdown. (F and G) TER and PNa^+/PCl^- responses of control and claudin-2 knockdown monolayers to CK2 inhibition. (H and I) TER and PNa^+/PCl^- responses of control, claudin-1, claudin-2, and double-knockdown monolayers to CK2 inhibition. (J) Tight junction protein expression in Caco-2 and T84 monolayers, before or after 12 h of IL-13 treatment (1 ng/ml). (K and L) Effect of CK2 inhibition (50 μM TBCA) on TER and PNa^+/PCl^- of control and IL-13–treated T84 monolayers.

(Fig. 6 E), and reduced paracellular permeability to cations smaller than ~2.5 Å (Fig. S4 C). In addition, claudin-2 knockdown monolayers displayed only limited TER increases (Fig. 6 F) and no change in Na^+ selectivity (Fig. 6 G) after CK2 inhibition. The small size of the TER increases was not due to global disruption of barrier regulatory mechanisms, as claudin-2 knockdown monolayers remained sensitive to myosin light chain kinase inhibition (Fig. S4 D). Therefore, in a manner that parallels FRAP and in vitro binding data, claudin-2 is required for CK2-mediated regulation of paracellular cation permeability.

Published May 2, 2011

The effect of CK2 inhibition on TER was markedly reduced by claudin-2 knockdown. Nevertheless, a slight, although statistically significant, increase in TER was induced by 50 µM TBCA (Fig. 6 F). This could reflect off-target effects of TBCA at higher doses, such as GSK3 inhibition (Pagano et al., 2007). However, the observations that occludin or ZO-1 knockdown completely blocked the effects of TBCA, even at 50 µM (Fig. 6, A–D), argue against this explanation. Given that claudin-1 recovery and FRAP behavior are also modulated by S408 dephosphorylation, it was reasonable to hypothesize that claudin-1 could be responsible for the residual effects of 50 µM TBCA on TER of claudin-2 knockdown monolayers. Transient claudin-1 knockdown (Fig. S4 E) increased baseline TER, but to a much smaller degree than claudin-2 knockdown (Fig. 6 E), suggesting that claudin-1 enhances paracellular permeability. However, claudin-1 knockdown in cells lacking claudin-2 reduced TER, relative to claudin-2 knockdown alone, suggesting that claudin-1 may enhance barrier function in some contexts. Thus, claudin-1 may have both pore-forming and barrier-sealing functions. Although further study is required, this interpretation could be consistent with diverse but poorly defined claudin-1 functions in enhancing barrier function of MDCK monolayers, endothelial monolayers, and mouse skin (Inai et al., 1999; Furuse et al., 2002; Fujibe et al., 2004), as well as preventing congenital liver and skin disease in human patients (Hadj-Rabia et al., 2004).

Much like claudin-2 knockdown, claudin-1 knockdown reduced, but did not eliminate TER increases after CK2 inhibition (Fig. 6 H). However, combined claudin-1 and claudin-2 knockdown completely prevented TER increases induced by CK2 inhibition (Fig. 6 H). In contrast, claudin-1 knockdown did not prevent CK2 inhibitor-induced PNa^+/PCl^- decreases, and charge selectivity responses of claudin-1/claudin-2 double knockdown monolayers were indistinguishable from those with only claudin-2 knockdown (Fig. 6 I). These data suggest that although claudin-1 contributes to CK2-mediated TER regulation, it participates by a mechanism that is distinct from claudin-2–dependent modulation of paracellular Na^+ pathway permeability.

CK2 inhibition corrects pathophysiologic barrier dysfunction

Claudin-2 expression is markedly up-regulated in inflammatory bowel disease (Heller et al., 2005; Prasad et al., 2005; Holmes et al., 2006), likely as a result of IL-13 signaling (Heller et al., 2005; Prasad et al., 2005; Fichtner-Feigl et al., 2006, 2008). This can be reproduced in vitro (Heller et al., 2005; Weber et al., 2010), but the effect is limited in Caco-2 monolayers, which express claudin-2 constitutively. In contrast, T84 intestinal epithelial cells normally possess little claudin-2, but IL-13 markedly up-regulates claudin-2 expression to reduce TER and increase PNa^+/PCl^- (Prasad et al., 2005; Weber et al., 2010). To determine if CK2 inhibition could correct IL-13–induced barrier dysfunction, T84 cells were treated with IL-13 to induce a 3.0 ± 0.2-fold increase in claudin-2 expression (Fig. 6 J), 23 ± 2% reduction in TER (Fig. 6 K), and 58 ± 11% increase in PNa^+/PCl^- (Fig. 6 L). Remarkably, subsequent CK2 inhibition completely reversed IL-13–induced TER loss (Fig. 6 K) and PNa^+/PCl^- increase (Fig. 6 L). Thus, CK2 inhibition can acutely reverse IL-13–induced barrier dysfunction and CK2 may be an attractive target for future pharmacological modulation of pathophysiological barrier defects.

Discussion

Despite a multitude of described interactions between TJ proteins, little information is available for understanding the means by which separate TJ components work together to regulate barrier function. Thus, identification of the molecular mechanisms that underlie TJ regulation is a major challenge that must be addressed during the next phase of TJ discovery. To begin to explore these processes, we assessed the effect of occludin phosphorylation on TJ molecular structure and barrier function. We focused on CK2, which acts as an occludin kinase in vivo and in vitro (Cordenonsi et al., 1997, 1999; Smales et al., 2003; Dörfel et al., 2009), but has not been associated with TJ regulation. The data show that CK2-mediated phosphorylation of occludin S408 modulates interactions between occludin, ZO-1, claudin-1, and claudin-2, and implicate S408 phosphorylation as a molecular switch that regulates TJ structure and paracellular pore pathway flux.

A model of CK2-mediated, occludin S408 phosphorylation-dependent barrier regulation

The data presented here show that CK2 inhibition reduces paracellular cation flux. This regulation requires occludin, and can be reproduced by S408A occludin expression without CK2 inhibition. ZO-1, claudin-1, and claudin-2 are also required for barrier regulation after CK2 inhibition, suggesting that occludin S408 dephosphorylation regulates claudin pore function via ZO-1 (Fig. 7). Thus, although we have focused on CK2, the phosphatase responsible for S408 dephosphorylation may also be important.

We used a combination of morphological and biochemical approaches to determine the mechanisms by which TJ proteins contribute to CK2-mediated barrier regulation. Morphometric analyses showed increased TJ localization of occludin after CK2 inhibition or S408A mutation. In binding assays, S408A occludin tail recovered more claudin-1 and claudin-2, but not claudin-4, from cell lysates, and also demonstrated enhanced ZO-1 binding, relative to a S408D mutant. Consistent with a role for ZO-1 as a scaffold, claudin-2 recovery from ZO-1 knockdown cell lysates was poor and similar for both occludin tails. Thus, static analyses of subcellular localization and in vitro binding suggest that S408 dephosphorylation promotes occludin trafficking to the TJ and physical association with ZO-1, claudin-1, and claudin-2.

Although a great deal has been learned from in vitro binding studies (Furuse et al., 1994; Itoh et al., 1997, 1999b; Fanning et al., 1998, 2002; Cordenonsi et al., 1999; Wittchen et al., 1999; Barritt et al., 2000; D'Atri and Citi, 2001; Meyer et al., 2002; Kale et al., 2003; Betanzos et al., 2004; Li et al., 2005; Müller et al., 2005; Seth et al., 2007; Van Itallie et al., 2008a), they do not provide information about dynamic interactions, are not generally used to measure protein interaction

Published May 2, 2011

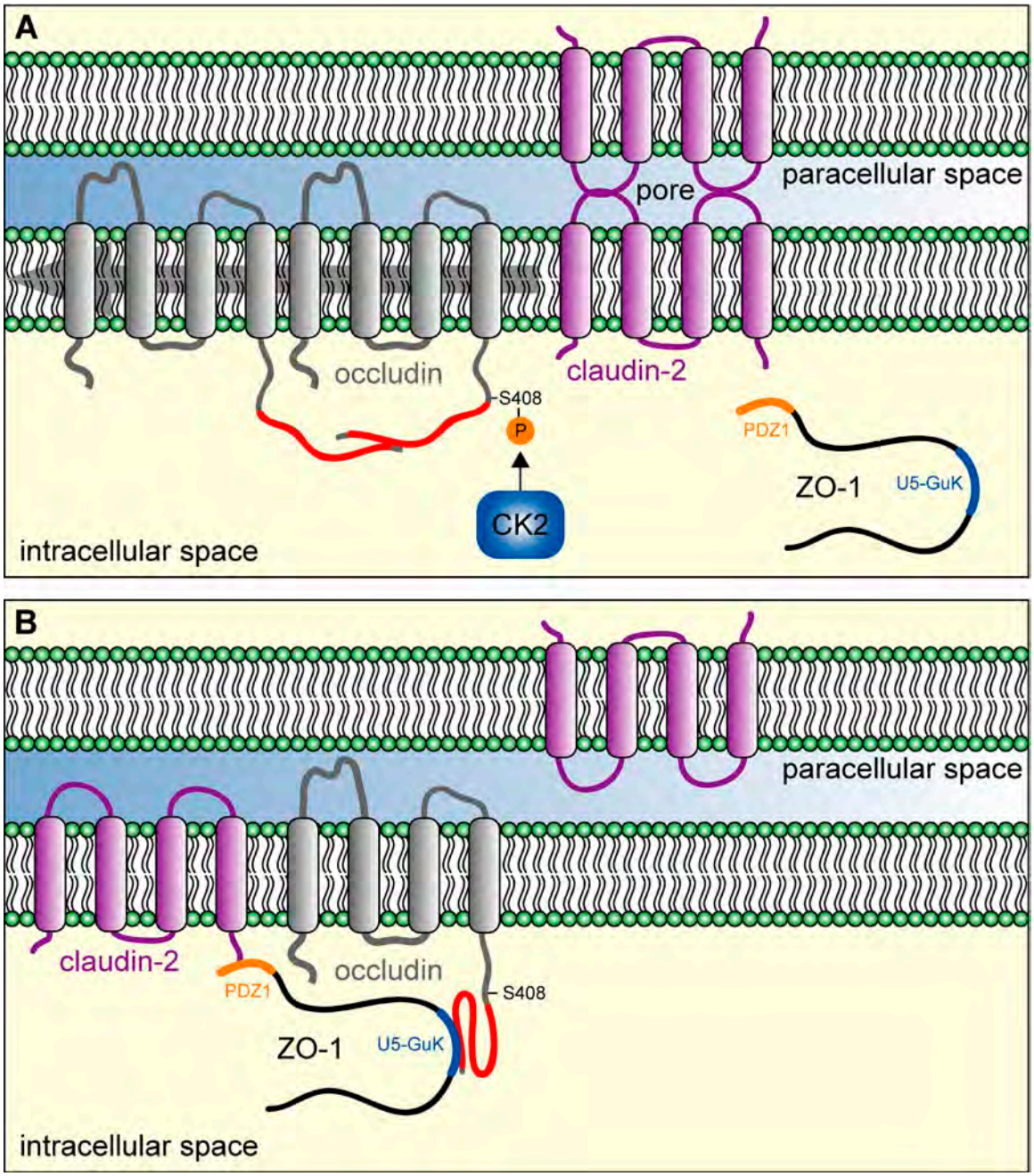

Figure 7. **Model of CK2-mediated regulation of TJ structure, dynamic behavior, and barrier function through occludin S408 phosphorylation.** Proposed organization, interactions, and dynamic behavior of proteins involved in TJ regulation by CK2. (A) CK2-mediated phosphorylation of S408 enhances occludin self-association, increases the occludin mobile fraction, and reduces occludin association with ZO-1, claudin-1, and claudin-2. This promotes flux across claudin-2, and, to a lesser extent, claudin-1 pores, thereby increasing paracellular cation flux. (B) When dephosphorylated at S408, occludin is stabilized at the TJ through enhanced association with ZO-1 via the U5-GuK domain. ZO-1 also facilitates indirect interactions between occludin and claudin-2, which associates with ZO-1 via the PDZ1 domain, thereby acting as a scaffold to organize a complex. As a result, dynamic behaviors of occludin, ZO-1, claudin-1, and claudin-2 converge, and function of claudin-1 and claudin-2 paracellular pores is reduced.

affinities, and cannot account for changes in protein structure or other regulatory events within live cells. We have therefore used mobile fraction as a measure of protein interactions in living cells. Although this is an indirect approach that has its own shortcomings, the combination of FRAP with in vitro binding data can be a powerful tool in analysis of protein interactions and function. Our studies show that both CK2 inhibition and S408A mutation reduce occludin mobile fraction, consistent with increased occludin localization at the TJ under these conditions. Although in vitro binding data show that occludin S408A mutation enhances occludin tail binding to ZO-1 and, via ZO-1, to claudin-1 and claudin-2, CK2 inhibition or S408A mutation increased mobile fractions of ZO-1 and these claudins. These data could be seen as contradictory, as one might presume that increased protein interactions should reduce the mobile fraction. However, this assumes that FRAP occurs entirely

Published May 2, 2011

by diffusion, which is not the case (Shen et al., 2008). Here, the in vitro binding and FRAP data can be resolved by a model in which occludin dimers form more readily after S408 phosphorylation and are more mobile within the TJ, perhaps because they are not anchored by ZO-1, whereas binding of occludin and ZO-1 after S408 dephosphorylation disrupts interactions that anchor ZO-1 and, in turn, some claudins (Fig. 7). This will be an important issue to address in the future.

Previous studies have correlated overall occludin hyperphosphorylation with TJ localization (Sakakibara et al., 1997; Wong, 1997). Although correct at a global level (Seth et al., 2007), this is not necessarily true of specific phosphorylation sites within the C-terminal occludin tail. For example, phosphorylation of T403 and T404 facilitates trafficking to the epithelial TJ (Suzuki et al., 2009), whereas phosphorylation of Y398 and Y402 interferes with ZO-1 binding and TJ trafficking (Elias et al., 2009), and S490 phosphorylation results in ubiquitination, endocytosis, and downstream endothelial barrier loss (Murakami et al., 2009; Sundstrom et al., 2009). Thus, phosphorylation of specific sites within the occludin C-terminal tail may either enhance or diminish occludin TJ localization and barrier function. Our results show that S408 phosphorylation decreases occludin localization and stability at the TJ and also reduces interactions with ZO-1. Conversely, S408 dephosphorylation, or mutation to alanine, stabilizes and increases the amount of occludin at the TJ, enhances interactions with ZO-1, promotes association with claudin-1 and claudin-2, and reduces paracellular ion flux. However, ZO-1 is required for occludin stabilization, claudin binding, and barrier regulation after S408 dephosphorylation, suggesting that physical interactions between occludin and ZO-1 are critical mediators of these events. Interestingly, similar to myosin light chain kinase-dependent control of barrier function (Yu et al., 2010) and integrity (Van Itallie et al., 2009a), but in contrast to TJ assembly (McNeil et al., 2006; Shin and Margolis, 2006; Umeda et al., 2006), ZO-2 cannot substitute for ZO-1 in occludin S408-mediated TJ regulation.

Although changes in steady-state distributions were not detected, FRAP studies revealed increases in ZO-1, claudin-1, and claudin-2 mobile fractions after CK2 inhibition and S408A mutation. This resulted in convergence of occludin, ZO-1, claudin-1, and claudin-2 mobile fractions after occludin S408 dephosphorylation, and, for claudin-2, required that ZO-1 contain both PDZ1 and U5-GuK domains. Further, in vitro binding studies showed enhanced association of ZO-1, claudin-1, and claudin-2 with S408A, relative to S408D, occludin tail. As a whole, these data strongly support the idea that S408 dephosphorylation facilitates assembly of a protein complex to regulate molecular structure and barrier properties of the TJ.

In contrast to claudin-1 and claudin-2, neither in vitro binding nor FRAP analyses detected any changes in claudin-4 after S408 dephosphorylation. Thus, in addition to differences within the first extracellular loop that define charge selectivity (Van Itallie et al., 2001; Colegio et al., 2002), other structural features that determine functional differences between claudins remain to be discovered. These may include extracellular determinants of cis or trans interactions between claudins (Daugherty et al., 2007; Lim et al., 2008a,b; Piontek et al., 2008; Piehl et al., 2010). However, because at least some of the interactions described here must occur within the cytoplasm, intracellular claudin domains (Itoh et al., 1999a; Hamazaki et al., 2002; Van Itallie et al., 2004, 2005; Tanaka et al., 2005), e.g., the N-terminal tail, intracellular loop, or C-terminal tail, should also be considered.

Mechanisms by which occludin S408 serves as a molecular switch

The residues phosphorylated by CK2, including S408, are located immediately upstream of the OCEL domain that mediates occludin self-association, ZO-1 binding, and interactions with other proteins (Furuse et al., 1994; Fanning et al., 1998; Nusrat et al., 2000; Li et al., 2005; Blasig et al., 2006). Occludin residues 416–522 form three α-helices with a positively charged surface that binds ZO-1; replacement of these residues with aspartic acid abolishes both binding to ZO-1 and occludin trafficking to cell contacts (Li et al., 2005). The data reported here and those reported by others suggest that phosphorylation events just proximal to the OCEL domain regulate occludin–ZO-1 interactions and occludin trafficking (Kale et al., 2003; Elias et al., 2009; Murakami et al., 2009; Suzuki et al., 2009). Specifically, our studies indicate that S408 functions as a molecular switch that determines whether occludin forms homodimers or heterotypic interactions with ZO-1 and, therefore, suggest that S408 phosphorylation regulates coiled-coil domain structure. However, although crystal structure of recombinant occludin tails composed of residues 383–522 or 416–522 has been reported (Li et al., 2005), these constructs were not phosphorylated and there is no information available to describe the effect of phosphorylation events on coiled-coil domain structure. Nevertheless, it is interesting to note that both recombinant occludin tails behaved as monomers (Li et al., 2005), consistent with our hypothesis that dephosphorylation of S408 prevents occludin self-association.

Occludin regulates leak and pore pathway function

Both in vitro and in vivo studies suggest that occludin is not required for TJ assembly or development of barrier function (Saitou et al., 2000; Schulzke et al., 2005; Yu et al., 2005). This has led some to conclude that occludin is either a regulatory protein or is wholly unimportant to TJ function. Consistent with the former interpretation, occludin has been implicated in regulation of leak pathway flux of large macromolecules by studies of occludin knockdown, overexpression, or mutation in MDCK monolayers (Balda et al., 1996; Yu et al., 2005). Moreover, recent in vitro and in vivo work has demonstrated a critical role for occludin in cytokine-dependent leak pathway regulation (Marchiando et al., 2010; Van Itallie et al., 2010). Given that the occludin tail binds directly to ZO-1, but not claudins, this also agrees with recent data showing that ZO-1 is required for leak pathway regulation (Van Itallie et al., 2009a). Our observation that occludin phosphorylation modifies permeability of claudin-based pores was, therefore, unexpected. Thus, these new data add to the functions assigned to occludin and show that, beyond regulating the TJ leak pathway, occludin also contributes to control of pore pathway permeability.

Published May 2, 2011

Potential therapeutic utility of CK2 inhibition and occludin S408 dephosphorylation

Our observation that occludin regulates paracellular pore function by a mechanism that is, primarily, dependent on claudin-2, together with the near complete absence of claudin-2 expression in adult mouse intestine (Holmes et al., 2006), is consistent with essentially normal intestinal Na^+ conductance and epithelial resistance reported in adult occludin knockout (Saitou et al., 2000; Schulzke et al., 2005) and adult, but not neonatal, claudin-2 knockout mice (Tamura et al., 2011). In addition, these data fit with the observations that CK2 inhibition reduces EGFP-occludin mobile fraction but does not affect paracellular flux of BSA, a leak pathway probe, or water in vivo. However, claudin-2 expression is known to be induced by mucosal immune activation in mice (Weber et al., 2010) and in human and experimental inflammatory bowel disease (Heller et al., 2005; Prasad et al., 2005; Zeissig et al., 2007; Weber et al., 2008, 2010). Our data show that, in this situation, CK2 inhibition reverses claudin-2–dependent increases in paracellular cation flux induced by IL-13, a key pathological mediator (Heller et al., 2002, 2005). Thus, although regulation of occludin S408 phosphorylation is not understood and would benefit from development of detection reagents, such as phosphospecific antibodies, it is tempting to speculate that CK2 inhibitors, several of which are being considered for clinical trials (Bortolato et al., 2008; Siddiqui-Jain et al., 2010), may be of therapeutic use in inflammatory bowel disease.

In conclusion, these data demonstrate that occludin S408 phosphorylation by CK2 acts as a molecular switch that regulates TJ protein interactions, molecular dynamics, and barrier function. In the absence of CK2 activity, occludin, ZO-1, and claudin-2 form a stable complex at the TJ. By phosphorylating S408, CK2 dissociates these proteins and facilitates cation flux across claudin-2–based pores. These results provide a new framework to understand the molecular interactions that regulate the TJ barrier in health and disease.

Materials and methods

Cell culture

Caco-2_{BBe} cells were maintained in DME (4.5 g glucose/l) with 10% FCS and 15 mM Hepes, pH 7.4. Subconfluent, rapidly growing cultures were trypsinized and plated at confluence on collagen-coated, 0.4-µm pore size, polycarbonate membrane Transwells (Corning). Media was replenished thrice weekly, and monolayers were studied 14 d after confluence, unless otherwise specified (Turner et al., 1997). T84 cells were maintained in 1:1 F12/RPMI1640 media supplemented with 10% newborn calf serum and 15 mM Hepes, pH 7.4, as described previously (Weber et al., 2010). These were plated at confluence on Transwell membranes and studied after 10 d. CK2 inhibitors used were 4,5,6,7-tetrabromobenzotriazole (Sigma-Aldrich), 2-dimethylamino-4,5,6,7-tetrabromo-1H-benzimidazole (Sigma-Aldrich), and tetrabromocinnamic acid (EMD). All CK2 inhibitor stocks were made in DMSO. DMAT became unavailable and was replaced by TBCA in the course of this work. CK2 inhibitors and S3226 (Aventis Pharma) were added to both apical and basolateral media (Schwark et al., 1998). PIK was applied apically (Zolotarevsky et al., 2002). IL-13 (R&D Systems) was added basally as described previously (Weber et al., 2010).

Electrophysiology and barrier function

A standard current clamp (University of Iowa Bioengineering, Iowa City, IA) was used to measure transepithelial resistance (TER) of cultured monolayers, as described previously (Turner et al., 1997). TER of control Caco-2 monolayers ranged from 151 ± 6 to 255 ± 5 Ohms x cm^2. All data shown are representative of ≥3 experiments, each in triplicate or greater. For stable transfectants, data are representative of ≥3 stable cell lines for each construct, each assayed in triplicate.

NaCl dilution potentials were measured similarly and ion selectivity was determined as described previously (Weber et al., 2010). Biionic potentials were measured by replacing basal Na, which has a radius of 0.95 Å, for organic cations with larger radii, specifically methylamine (1.9 Å), ethylamine (2.3 Å), tetramethylammonium (2.8 Å), tetraethylammonium (3.3 Å), or N-methyl-D-glucamine (3.7 Å) (Sigma-Aldrich). Absolute Na^+ permeability (P_{Na}) was calculated using the equation

$$PNa = \frac{RT}{F^2} \times \frac{G}{[Na^+] + \frac{PCl}{PNA}[Cl^-]},$$

where G is the overall monolayer conductance per unit surface area measured in symmetrical HBSS solutions, R is the absolute temperature, R is the gas constant, and F is Faraday's constant (Kimizuka and Koketsu, 1964; Yu et al., 2009). From the value of P_{Na}, and the known relative permeabilities to the other ions, the absolute permeabilities to those ions could then be deduced using the Goldman-Hodgkin-Katz equation. Liquid junction potentials, measured using cell-free Transwells, were <0.1 mV. All data shown are representative of ≥3 experiments, each in triplicate.

For flux of larger macromolecules, FITC (0.1 mg/ml), 3-kD FITC-dextran (1 mg/ml), and 10-kD FITC-dextran (2.5 mg/ml) conjugates (Invitrogen) were added to the apical chamber. Aliquots were removed from the basal chamber at 30-min intervals over 2 h, as described previously (Wang et al., 2005). All data shown are representative of ≥3 experiments, each in triplicate.

Gene knockdown

For transient CK2 knockdown, Caco-2_{BBe} cells were cotransfected with pooled CK2α (5′-GCAUUUAGGUGGAGACUUC-3′, 5′-GGAAGUGUCUUAGUUAC-3′, 5′-GCUGGUCGCUUACAUCACU-3′, and 5′-AACAUUGUCUGUACAGGUU-3′) and CK2α′ (5′-GAGUUUGGGCUGUAUGUUA-3′, 5′-GGGACAACAUUCACGGAAA-3′, 5′-GAUAGAUCACCAACAGAAA-3′, and 5′-UUAAGCAACUCUACCAGAU-3′) targeting siRNA (Thermo Fisher Scientific). Transient claudin-1 knockdown used pooled claudin-1 (5′-GAGGAUGGCUGUCAUUGGG-3′, 5′-CACCAAGGCCCUAUCCAAA-3′, 5′-GGAAAGACUACGUGUGACA-3′, and 5′-GCAAUAGAAUCGUUCAAGA-3′) targeting siRNA (Thermo Fisher Scientific). All siRNA species were transfected using Lipfectamine 2000 (Invitrogen), as described previously (Hu et al., 2006), and controls were transfected with nontargeting pooled scrambled siRNAs with similar GC content. Monolayers were studied 7 d after confluence.

pSUPER (Oligoengine) containing the occludin targeting sequence 5′-GTGAAGAGTACATGGCTGC-3′ (Yu et al., 2005) was used to stably transfect Caco-2_{BBe} cells stably expressing SGLT1 (Turner et al., 1997), which suppressed >90% of occludin expression. ZO-1 knockdown cells were generated similarly, as described previously (Yu et al., 2010). Claudin-2 knockdown was achieved by stably transfecting Caco-2_{BBe} with pSUPER vector containing the targeting sequence 5′-GCTAAGGGCTATAGACAAT-3′. Controls for each were stably transfected with a pSUPER vector containing a related, but ineffective, sequence.

CK2 assay

CK2 activity was assessed in lysates of siRNA-treated Caco-2 cells as described previously (Ruzzene et al., 2010). In brief, 300 µg total cell protein was incubated with 0.1 mM CK2 substrate peptide (RRRADDSDDDDD) and 10 µM [^{32}P]ATP for 10 min at 30°C in a total volume of 20 µl. Reactions were terminated by spotting onto phosphocellulose filters, which were then washed with 0.5% phosphoric acid. Because other kinases can phosphorylate the substrate peptide, all samples were assayed in the presence of vehicle or 0.5 µM TBCA; the TBCA-inhibitable activity was considered to represent CK2 activity.

Immunoblots

Caco-2_{BBe} monolayers were scraped from Transwell supports and mouse jejunal enterocytes were isolated as described previously (Clayburgh et al., 2005; Raleigh et al., 2010). Cells were resuspended and lysed in reducing Laemmli sample buffer, and protein concentrations were determined. Equal quantities of protein were loaded into each lane for SDS-PAGE separation. Immunoblots were performed as described previously (Raleigh et al., 2010),

Published May 2, 2011

using CK2α (BD), CK2α′ (Abcam), claudin-1, claudin-2, claudin-4, occludin, tricellulin, ZO-1, ZO-2, and GAPDH antibodies (Invitrogen), as well as anti-marvelD3 (Raleigh et al., 2010) polyclonal antisera, and anti-VSVG monoclonal antibodies (Kreis, 1986).

Immunofluorescent staining and microscopy

To preserve intracellular vesicles, monolayers were fixed at −20°C with methanol and then cross-linked with bis(sulfosuccinimidyl)suberate (Shen and Turner, 2005). Immunofluorescent staining used GFP, claudin-1, claudin-2, claudin-4, occludin, tricellulin, and ZO-1 antibodies (Invitrogen), as well as anti-marvelD3 (Raleigh et al., 2010) polyclonal antisera and CK2α antibodies (BD), followed by species-specific secondary antisera conjugated to Alexa Fluor 488 or Alexa Fluor 594 (Invitrogen). Images were collected using a DMLB epifluorescence microscope (Leica) equipped with an 88000 filter set (Chroma Technology Corp.), a 63x Plan Apochromat 1.32 NA oil immersion objective, Retiga EXi camera (QImaging), and controlled by MetaMorph 7. Z stacks were collected at 0.2-µm intervals, and deconvolved with Autodeblur X2 (Media Cybernetics) for 10 iterations, with low noise level, intensity correction, accelerated SA detection, minimal intensity removal, and dynamic subvoluming as described previously (Raleigh et al., 2010). All images shown are representative of ≥3 independent experiments, each with at least duplicate samples. For morphometric analyses, TJ intensity was calculated as the ratio of TJ to total cell fluorescence, using at least 30 cells from each of three independent experiments (for each treatment condition).

Fluorescent proteins

Fluorescent fusion constructs were generated as described previously (Campbell et al., 2002; Shen and Turner, 2005; Raleigh et al., 2010). Claudin-2 (I.M.A.G.E. clone 30322852) and claudin-4 (I.M.A.G.E. clone 3349211) cDNAs were purchased from American Type Culture Collection (Manassas, VA). Site-directed mutagenesis with the QuikChange XL kit (Agilent Technologies) was used to create serine to alanine, serine to aspartic acid, and silent siRNA-evading mutations within EGFP-occludin. Wild-type EGFP-ZO-1 with silent siRNA-evading mutations for reexpression in ZO-1 knockdown cells was generated by site-directed mutagenesis; amino acids 1–120 and 590–803 were eliminated to create EGFP-ZO-1 ΔPDZ1 and ΔU5-GuK mutant constructs, respectively. Sequencing and restriction digestion was used to confirm plasmid sequence and directionality.

FRAP

In vitro FRAP was performed after transfection of fluorescent constructs into Caco-2_{BBe} cells as described previously (Raleigh et al., 2010; Yu et al., 2010), and, where indicated, after 3 h of treatment with either pharmacological CK2 inhibitors or vehicle. Monolayers were imaged in HBSS supplemented with drug or vehicle on a 37°C temperature-controlled stage. Fluorescence bleaching and imaging were performed using an epifluorescence microscope (model DM4000; Leica) with a MicroPoint system (Photonic Instruments), Coolsnap HQ camera (Roper Scientific), and 63x U-V-I 1.2 NA water immersion objective controlled by MetaMorph 7. Images were collected until steady-state fluorescence intensity was reached. All data shown are representative of ≥3 experiments, each with $n = 4$.

In vivo FRAP was performed after intestinal perfusion of DMAT or vehicle (see below), as described previously (Yu et al., 2010). EGFP-occludin was excited using a 488 argon ion laser mounted on an SP5 microscope (Leica) with a 40x 0.8 NA water immersion objective. Bleaching was performed with 476, 488, and 514 argon ion lasers, and images were collected until steady-state fluorescence intensity was reached. Data for in vivo FRAP data are displayed as the average of ≥40 bleach sites per mouse, with two mice studied for each condition.

Raw data were aligned and mean fluorescence of background, whole-field, and bleached regions were quantified over time using MetaMorph. Background fluorescence was subtracted from bleached regions and whole-field fluorescence at each time point. Bleached region and whole-field data were normalized to their respective prebleach intensities, and fluorescence recovery within bleached regions relative to whole-field intensity was plotted over time. Sigma Plot (SPSS Inc.) was used for curve fitting to $f(x) = y_0 + a(1 - e^{-bx})$. Mobile fraction and halftime of recovery were calculated as $(a)/(1 - y_0)$ and $ln(2)/b$, respectively. Neither occludin mutation nor CK2 inhibition altered $t_{1/2}$ of recovery, in vitro or in vivo.

Animals

Experiments were performed using 7–10-wk-old C57BL/6 mice expressing EGFP-occludin under control of the villin promoter (Marchiando et al., 2010). All studies were conducted in an AAALAC accredited facility under protocols approved by The University of Chicago IACUC. For in vivo CK2 inhibition, mice were anaesthetized and a 5-cm loop of jejunum was exposed, cannulated, and flushed to remove luminal material. The jejunum was perfused with media containing DMAT or vehicle for 60 min before imaging as described previously (Marchiando et al., 2010). A similar approach was used to assess paracellular Alexa 488 BSA and water flux in vivo (Clayburgh et al., 2005; Marchiando et al., 2010).

GST pulldown

GST-occludin 383–522 wild-type, S408D, and S408A constructs were generated by site-directed mutagenesis of previously described GST-occludin C-terminal tail constructs (Raleigh et al., 2010). A VSV G epitope-tagged human ZO-1 U5-GuK domain construct consisting of residues 591–754 was generated by cloning cDNA into pGEX-4T3 (GE Healthcare) and removing the GST coding sequence by site-directed mutagenesis (Raleigh et al., 2010). BL21(DE3)pLysS-competent bacteria were transformed with GST- and VSV G–tagged constructs, induced with IPTG, and processed using a GST Protein Interaction Pulldown kit (Thermo Fisher Scientific) with RIPA buffer containing TBS, 1% Nonidet P-40, 0.5% sodium deoxycholate, 0.1% SDS, 0.004% sodium azide, and protease and phosphatase inhibitors (Santa Cruz Biotechnology, Inc.). For pulldown from Caco-2_{BBe} lysates, monolayers were washed once in 4°C TBS and incubated in RIPA buffer at 4°C for 30 min. Cells were passed five times through a 21-gauge needle, and clarified for 5 min at 12,000 rpm. Bacterial and Caco-2_{BBe} supernatants were incubated with immobilized bait constructs at 4°C overnight with rocking, and, after three washes in 10 mM NaCl, eluted with 10 mM reduced glutathione. All data shown are representative of ≥2 experiments, each with at least duplicate samples.

Statistical analysis

All data are presented as mean ± SE unless otherwise specified. Student's unpaired *t* test was used to compare means, with statistical significance taken as $P < 0.05$.

Online supplemental material

Fig. S1 shows that neither CK2 inhibition nor CK2 knockdown affect TJ protein expression, provides controls for CK2 knockdown, demonstrates that CK2 effects on NHE3 function do not play a role in the observed barrier regulation, assesses paracellular flux of larger uncharged molecules before and after CK2 inhibition, and evaluates intracellular CK2 distribution. Fig. S2 shows kymographs of EGFP-occludin in control and CK2 knockdown Caco-2 monolayers, images and kymographs of EGFP-occludin in mouse jejunal enterocytes in vivo, that CK2 inhibition does not affect TJ protein expression in mouse jejunal enterocytes, and that CK2 inhibition does not affect in vivo water transport or paracellular BSA flux in mouse jejunum. Fig. S3 shows redistribution of wild-type and mutant EGFP-occludin proteins in response to CK2 inhibition and provides protein expression and transepithelial resistance data for transfected Caco-2 monolayers. Fig. S4 shows protein expression after ZO-1, claudin-1, or claudin-2 knockdown, cation permeability of stable claudin-2 knockdown Caco-2 cell lines, and the TER response of claudin-2 knockdown cell lines to myosin light chain kinase inhibition. Online supplemental material is available at http://www.jcb.org/cgi/content/full/jcb.201010065/DC1.

We thank Lindsay Raleigh for support and encouragement; W. Vallen Graham, Andrew Hawk, Stephen C. Meredith, Adam Schmitt, and Alan Yu for generously sharing advice; and Juergen Puenter and Roger Tsien for providing essential reagents.

This work was supported by the National Institutes of Health grants R01DK61931, R01DK68271, P01DK67887, P30CA14599, P30DK042086, K08DK088953, T32HL007237, T32DK007074, and T32GM07281. L. Shen is supported by a Crohn's and Colitis Foundation of America Career Development Award and was previously supported by a Crohn's and Colitis Foundation of America Research Fellowship Award sponsored by Ms. Laura McAteer Hoffman.

Submitted: 13 October 2010
Accepted: 29 March 2011

References

Amasheh, S., N. Meiri, A.H. Gitter, T. Schöneberg, J. Mankertz, J.D. Schulzke, and M. Fromm. 2002. Claudin-2 expression induces cation-selective channels in tight junctions of epithelial cells. *J. Cell Sci.* 115:4969–4976. doi:10.1242/jcs.00165

Anderson, J.M., and C.M. Van Itallie. 2009. Physiology and function of the tight junction. *Cold Spring Harb. Perspect. Biol.* 1:a002584. doi:10.1101/cshperspect.a002584

Angelow, S., E.E. Schneeberger, and A.S. Yu. 2007. Claudin-8 expression in renal epithelial cells augments the paracellular barrier by replacing endogenous claudin-2. *J. Membr. Biol.* 215:147–159. doi:10.1007/s00232-007-9014-3

Balda, M.S., J.A. Whitney, C. Flores, S. González, M. Cereijido, and K. Matter. 1996. Functional dissociation of paracellular permeability and transepithelial electrical resistance and disruption of the apical-basolateral intramembrane diffusion barrier by expression of a mutant tight junction membrane protein. *J. Cell Biol.* 134:1031–1049. doi:10.1083/jcb.134.4.1031

Balda, M.S., C. Flores-Maldonado, M. Cereijido, and K. Matter. 2000. Multiple domains of occludin are involved in the regulation of paracellular permeability. *J. Cell. Biochem.* 78:85–96. doi:10.1002/(SICI)1097-4644(20000701)78:1<85::AID-JCB8>3.0.CO;2-F

Barritt, D.S., M.T. Pearn, A.H. Zisch, S.S. Lee, R.T. Javier, E.B. Pasquale, and W.B. Stallcup. 2000. The multi-PDZ domain protein MUPP1 is a cytoplasmic ligand for the membrane-spanning proteoglycan NG2. *J. Cell. Biochem.* 79:213–224. doi:10.1002/1097-4644(20001101)79:2<213::AID-JCB50>3.0.CO;2-G

Betanzos, A., M. Huerta, E. Lopez-Bayghen, E. Azuara, J. Amerena, and L. González-Mariscal. 2004. The tight junction protein ZO-2 associates with Jun, Fos and C/EBP transcription factors in epithelial cells. *Exp. Cell Res.* 292:51–66. doi:10.1016/j.yexcr.2003.08.007

Blasig, I.E., L. Winkler, B. Lassowski, S.L. Mueller, N. Zuleger, E. Krause, G. Krause, K. Gast, M. Kolbe, and J. Piontek. 2006. On the self-association potential of transmembrane tight junction proteins. *Cell. Mol. Life Sci.* 63:505–514. doi:10.1007/s00018-005-5472-x

Bortolato, A., G. Cozza, and S. Moro. 2008. Protein kinase CK2 inhibitors: emerging anticancer therapeutic agents? *Anticancer. Agents Med. Chem.* 8:798–806.

Campbell, R.E., O. Tour, A.E. Palmer, P.A. Steinbach, G.S. Baird, D.A. Zacharias, and R.Y. Tsien. 2002. A monomeric red fluorescent protein. *Proc. Natl. Acad. Sci. USA*. 99:7877–7882. doi:10.1073/pnas.082243699

Claude, P. 1978. Morphological factors influencing transepithelial permeability: a model for the resistance of the zonula occludens. *J. Membr. Biol.* 39:219–232. doi:10.1007/BF01870332

Claude, P., and D.A. Goodenough. 1973. Fracture faces of zonulae occludentes from "tight" and "leaky" epithelia. *J. Cell Biol.* 58:390–400. doi:10.1083/jcb.58.2.390

Clayburgh, D.R., T.A. Barrett, Y. Tang, J.B. Meddings, L.J. Van Eldik, D.M. Watterson, L.L. Clarke, R.J. Mrsny, and J.R. Turner. 2005. Epithelial myosin light chain kinase-dependent barrier dysfunction mediates T cell activation-induced diarrhea in vivo. *J. Clin. Invest.* 115:2702–2715. doi:10.1172/JCI24970

Colegio, O.R., C.M. Van Itallie, H.J. McCrea, C. Rahner, and J.M. Anderson. 2002. Claudins create charge-selective channels in the paracellular pathway between epithelial cells. *Am. J. Physiol. Cell Physiol.* 283:C142–C147.

Colegio, O.R., C. Van Itallie, C. Rahner, and J.M. Anderson. 2003. Claudin extracellular domains determine paracellular charge selectivity and resistance but not tight junction fibril architecture. *Am. J. Physiol. Cell Physiol.* 284:C1346–C1354.

Cordenonsi, M., E. Mazzon, L. De Rigo, S. Baraldo, F. Meggio, and S. Citi. 1997. Occludin dephosphorylation in early development of Xenopus laevis. *J. Cell Sci.* 110:3131–3139.

Cordenonsi, M., F. Turco, F. D'atri, E. Hammar, G. Martinucci, F. Meggio, and S. Citi. 1999. Xenopus laevis occludin. Identification of in vitro phosphorylation sites by protein kinase CK2 and association with cingulin. *Eur. J. Biochem.* 264:374–384. doi:10.1046/j.1432-1327.1999.00616.x

D'Atri, F., and S. Citi. 2001. Cingulin interacts with F-actin in vitro. *FEBS Lett.* 507:21–24. doi:10.1016/S0014-5793(01)02936-2

Daugherty, B.L., C. Ward, T. Smith, J.D. Ritzenthaler, and M. Koval. 2007. Regulation of heterotypic claudin compatibility. *J. Biol. Chem.* 282:30005–30013. doi:10.1074/jbc.M703547200

Dörfel, M.J., J.K. Westphal, and O. Huber. 2009. Differential phosphorylation of occludin and tricellulin by CK2 and CK1. *Ann. N. Y. Acad. Sci.* 1165:69–73. doi:10.1111/j.1749-6632.2009.04043.x

Elias, B.C., T. Suzuki, A. Seth, F. Giorgianni, G. Kale, L. Shen, J.R. Turner, A. Naren, D.M. Desiderio, and R. Rao. 2009. Phosphorylation of Tyr-398 and Tyr-402 in occludin prevents its interaction with ZO-1 and destabilizes its assembly at the tight junctions. *J. Biol. Chem.* 284:1559–1569. doi:10.1074/jbc.M804783200

Fanning, A.S., B.J. Jameson, L.A. Jesaitis, and J.M. Anderson. 1998. The tight junction protein ZO-1 establishes a link between the transmembrane protein occludin and the actin cytoskeleton. *J. Biol. Chem.* 273:29745–29753. doi:10.1074/jbc.273.45.29745

Fanning, A.S., T.Y. Ma, and J.M. Anderson. 2002. Isolation and functional characterization of the actin binding region in the tight junction protein ZO-1. *FASEB J.* 16:1835–1837.

Fanning, A.S., B.P. Little, C. Rahner, D. Utepbergenov, Z. Walther, and J.M. Anderson. 2007. The unique-5 and -6 motifs of ZO-1 regulate tight junction strand localization and scaffolding properties. *Mol. Biol. Cell*. 18:721–731. doi:10.1091/mbc.E06-08-0764

Fichtner-Feigl, S., W. Strober, K. Kawakami, R.K. Puri, and A. Kitani. 2006. IL-13 signaling through the IL-13alpha2 receptor is involved in induction of TGF-beta1 production and fibrosis. *Nat. Med.* 12:99–106. doi:10.1038/nm1332

Fichtner-Feigl, S., C.A. Young, A. Kitani, E.K. Geissler, H.J. Schlitt, and W. Strober. 2008. IL-13 signaling via IL-13R alpha2 induces major downstream fibrogenic factors mediating fibrosis in chronic TNBS colitis. *Gastroenterology*. 135:2003–2013: 2013: e1–e7. doi:10.1053/j.gastro.2008.08.055

Fujibe, M., H. Chiba, T. Kojima, T. Soma, T. Wada, T. Yamashita, and N. Sawada. 2004. Thr203 of claudin-1, a putative phosphorylation site for MAP kinase, is required to promote the barrier function of tight junctions. *Exp. Cell Res.* 295:36–47. doi:10.1016/j.yexcr.2003.12.014

Furuse, M., M. Itoh, T. Hirase, A. Nagafuchi, S. Yonemura, S. Tsukita, and S. Tsukita. 1994. Direct association of occludin with ZO-1 and its possible involvement in the localization of occludin at tight junctions. *J. Cell Biol.* 127:1617–1626. doi:10.1083/jcb.127.6.1617

Furuse, M., K. Furuse, H. Sasaki, and S. Tsukita. 2001. Conversion of zonulae occludentes from tight to leaky strand type by introducing claudin-2 into Madin-Darby canine kidney I cells. *J. Cell Biol.* 153:263–272. doi:10.1083/jcb.153.2.263

Furuse, M., M. Hata, K. Furuse, Y. Yoshida, A. Haratake, Y. Sugitani, T. Noda, A. Kubo, and S. Tsukita. 2002. Claudin-based tight junctions are crucial for the mammalian epidermal barrier: a lesson from claudin-1-deficient mice. *J. Cell Biol.* 156:1099–1111. doi:10.1083/jcb.200110122

Hadj-Rabia, S., L. Baala, P. Vabres, D. Hamel-Teillac, E. Jacquemin, M. Fabre, S. Lyonnet, Y. De Prost, A. Munnich, M. Hadchouel, and A. Smahi. 2004. Claudin-1 gene mutations in neonatal sclerosing cholangitis associated with ichthyosis: a tight junction disease. *Gastroenterology*. 127:1386–1390. doi:10.1053/j.gastro.2004.07.022

Hamazaki, Y., M. Itoh, H. Sasaki, M. Furuse, and S. Tsukita. 2002. Multi-PDZ domain protein 1 (MUPP1) is concentrated at tight junctions through its possible interaction with claudin-1 and junctional adhesion molecule. *J. Biol. Chem.* 277:455–461. doi:10.1074/jbc.M109005200

Heller, F., I.J. Fuss, E.E. Nieuwenhuis, R.S. Blumberg, and W. Strober. 2002. Oxazolone colitis, a Th2 colitis model resembling ulcerative colitis, is mediated by IL-13-producing NK-T cells. *Immunity*. 17:629–638. doi:10.1016/S1074-7613(02)00453-3

Heller, F., P. Florian, C. Bojarski, J. Richter, M. Christ, B. Hillenbrand, J. Mankertz, A.H. Gitter, N. Bürgel, M. Fromm, et al. 2005. Interleukin-13 is the key effector Th2 cytokine in ulcerative colitis that affects epithelial tight junctions, apoptosis, and cell restitution. *Gastroenterology*. 129:550–564.

Holmes, J.L., C.M. Van Itallie, J.E. Rasmussen, and J.M. Anderson. 2006. Claudin profiling in the mouse during postnatal intestinal development and along the gastrointestinal tract reveals complex expression patterns. *Gene Expr. Patterns*. 6:581–588. doi:10.1016/j.modgep.2005.12.001

Hu, Z., Y. Wang, W.V. Graham, L. Su, M.W. Musch, and J.R. Turner. 2006. MAPKAPK-2 is a critical signaling intermediate in NHE3 activation following Na^+-glucose cotransport. *J. Biol. Chem.* 281:24247–24253. doi:10.1074/jbc.M602898200

Inai, T., J. Kobayashi, and Y. Shibata. 1999. Claudin-1 contributes to the epithelial barrier function in MDCK cells. *Eur. J. Cell Biol.* 78:849–855.

Itoh, M., A. Nagafuchi, S. Moroi, and S. Tsukita. 1997. Involvement of ZO-1 in cadherin-based cell adhesion through its direct binding to alpha catenin and actin filaments. *J. Cell Biol.* 138:181–192. doi:10.1083/jcb.138.1.181

Itoh, M., M. Furuse, K. Morita, K. Kubota, M. Saitou, and S. Tsukita. 1999a. Direct binding of three tight junction-associated MAGUKs, ZO-1, ZO-2, and ZO-3, with the COOH termini of claudins. *J. Cell Biol.* 147:1351–1363. doi:10.1083/jcb.147.6.1351

Itoh, M., K. Morita, and S. Tsukita. 1999b. Characterization of ZO-2 as a MAGUK family member associated with tight as well as adherens junctions with a binding affinity to occludin and alpha catenin. *J. Biol. Chem.* 274:5981–5986. doi:10.1074/jbc.274.9.5981

Kale, G., A.P. Naren, P. Sheth, and R.K. Rao. 2003. Tyrosine phosphorylation of occludin attenuates its interactions with ZO-1, ZO-2, and ZO-3. *Biochem. Biophys. Res. Commun.* 302:324–329. doi:10.1016/S0006-291X(03)00167-0

Kimizuka, H., and K. Koketsu. 1964. Ion transport through cell membrane. *J. Theor. Biol.* 6:290–305. doi:10.1016/0022-5193(64)90035-9

Kreis, T.E. 1986. Microinjected antibodies against the cytoplasmic domain of vesicular stomatitis virus glycoprotein block its transport to the cell surface. *EMBO J.* 5:931–941.

Li, Y., A.S. Fanning, J.M. Anderson, and A. Lavie. 2005. Structure of the conserved cytoplasmic C-terminal domain of occludin: identification of the ZO-1 binding surface. *J. Mol. Biol.* 352:151–164. doi:10.1016/j.jmb.2005.07.017

Lim, T.S., S.R. Vedula, W. Hunziker, and C.T. Lim. 2008a. Kinetics of adhesion mediated by extracellular loops of claudin-2 as revealed by single-molecule force spectroscopy. *J. Mol. Biol.* 381:681–691. doi:10.1016/j.jmb.2008.06.009

Lim, T.S., S.R. Vedula, P.J. Kausalya, W. Hunziker, and C.T. Lim. 2008b. Single-molecular-level study of claudin-1-mediated adhesion. *Langmuir*. 24:490–495. doi:10.1021/la702436x

Litchfield, D.W., D.G. Bosc, D.A. Canton, R.B. Saulnier, G. Vilk, and C. Zhang. 2001. Functional specialization of CK2 isoforms and characterization of isoform-specific binding partners. *Mol. Cell. Biochem.* 227:21–29. doi:10.1023/A:1013188101465

Marchiando, A.M., L. Shen, W.V. Graham, C.R. Weber, B.T. Schwarz, J.R. Austin II, D.R. Raleigh, Y. Guan, A.J. Watson, M.H. Montrose, and J.R. Turner. 2010. Caveolin-1-dependent occludin endocytosis is required for TNF-induced tight junction regulation in vivo. *J. Cell Biol.* 189:111–126. doi:10.1083/jcb.200902153

McNeil, E., C.T. Capaldo, and I.G. Macara. 2006. Zonula occludens-1 function in the assembly of tight junctions in Madin-Darby canine kidney epithelial cells. *Mol. Biol. Cell*. 17:1922–1932. doi:10.1091/mbc.E05-07-0650

Meggio, F., and L.A. Pinna. 2003. One-thousand-and-one substrates of protein kinase CK2? *FASEB J.* 17:349–368. doi:10.1096/fj.02-0473rev

Meyer, T.N., C. Schwesinger, and B.M. Denker. 2002. Zonula occludens-1 is a scaffolding protein for signaling molecules. Galpha(12) directly binds to the Src homology 3 domain and regulates paracellular permeability in epithelial cells. *J. Biol. Chem.* 277:24855–24858. doi:10.1074/jbc.C200240200

Mitic, L.L., and J.M. Anderson. 1998. Molecular architecture of tight junctions. *Annu. Rev. Physiol.* 60:121–142. doi:10.1146/annurev.physiol.60.1.121

Müller, S.L., M. Portwich, A. Schmidt, D.I. Utepbergenov, O. Huber, I.E. Blasig, and G. Krause. 2005. The tight junction protein occludin and the adherens junction protein alpha-catenin share a common interaction mechanism with ZO-1. *J. Biol. Chem.* 280:3747–3756. doi:10.1074/jbc.M411365200

Murakami, T., E.A. Felinski, and D.A. Antonetti. 2009. Occludin phosphorylation and ubiquitination regulate tight junction trafficking and vascular endothelial growth factor-induced permeability. *J. Biol. Chem.* 284:21036–21046. doi:10.1074/jbc.M109.016766

Muto, S., M. Hata, J. Taniguchi, S. Tsuruoka, K. Moriwaki, M. Saitou, K. Furuse, H. Sasaki, A. Fujimura, M. Imai, et al. 2010. Claudin-2-deficient mice are defective in the leaky and cation-selective paracellular permeability properties of renal proximal tubules. *Proc. Natl. Acad. Sci. USA*. 107:8011–8016. doi:10.1073/pnas.0912901107

Nusrat, A., J.A. Chen, C.S. Foley, T.W. Liang, J. Tom, M. Cromwell, C. Quan, and R.J. Mrsny. 2000. The coiled-coil domain of occludin can act to organize structural and functional elements of the epithelial tight junction. *J. Biol. Chem.* 275:29816–29822. doi:10.1074/jbc.M002450200

Pagano, M.A., F. Meggio, M. Ruzzene, M. Andrzejewska, Z. Kazimierczuk, and L.A. Pinna. 2004. 2-Dimethylamino-4,5,6,7-tetrabromo-1H-benzimidazole: a novel powerful and selective inhibitor of protein kinase CK2. *Biochem. Biophys. Res. Commun.* 321:1040–1044. doi:10.1016/j.bbrc.2004.07.067

Pagano, M.A., G. Poletto, G. Di Maira, G. Cozza, M. Ruzzene, S. Sarno, J. Bain, M. Elliott, S. Moro, G. Zagotto, et al. 2007. Tetrabromocinnamic acid (TBCA) and related compounds represent a new class of specific protein kinase CK2 inhibitors. *ChemBioChem*. 8:129–139. doi:10.1002/cbic.200600293

Piehl, C., J. Piontek, J. Cording, H. Wolburg, and I.E. Blasig. 2010. Participation of the second extracellular loop of claudin-5 in paracellular tightening against ions, small and large molecules. *Cell. Mol. Life Sci.* 67:2131–2140. doi:10.1007/s00018-010-0332-8

Piontek, J., L. Winkler, H. Wolburg, S.L. Müller, N. Zuleger, C. Piehl, B. Wiesner, G. Krause, and I.E. Blasig. 2008. Formation of tight junction: determinants of homophilic interaction between classic claudins. *FASEB J.* 22:146–158. doi:10.1096/fj.07-8319com

Prasad, S., R. Mingrino, K. Kaukinen, K.L. Hayes, R.M. Powell, T.T. MacDonald, and J.E. Collins. 2005. Inflammatory processes have differential effects on claudins 2, 3 and 4 in colonic epithelial cells. *Lab. Invest.* 85:1139–1162. doi:10.1038/labinvest.3700316

Raleigh, D.R., A.M. Marchiando, Y. Zhang, L. Shen, H. Sasaki, Y. Wang, M. Long, and J.R. Turner. 2010. Tight junction-associated MARVEL proteins marveld3, tricellulin, and occludin have distinct but overlapping functions. *Mol. Biol. Cell*. 21:1200–1213. doi:10.1091/mbc.E09-08-0734

Rosenthal, R., S. Milatz, S.M. Krug, B. Oelrich, J.D. Schulzke, S. Amasheh, D. Günzel, and M. Fromm. 2010. Claudin-2, a component of the tight junction, forms a paracellular water channel. *J. Cell Sci.* 123:1913–1921. doi:10.1242/jcs.060665

Ruzzene, M., G. Di Maira, K. Tosoni, and L.A. Pinna. 2010. Assessment of CK2 constitutive activity in cancer cells. *Methods Enzymol.* 484:495–514. doi:10.1016/B978-0-12-381298-8.00024-1

Saitou, M., M. Furuse, H. Sasaki, J.D. Schulzke, M. Fromm, H. Takano, T. Noda, and S. Tsukita. 2000. Complex phenotype of mice lacking occludin, a component of tight junction strands. *Mol. Biol. Cell*. 11:4131–4142.

Sakakibara, A., M. Furuse, M. Saitou, Y. Ando-Akatsuka, and S. Tsukita. 1997. Possible involvement of phosphorylation of occludin in tight junction formation. *J. Cell Biol.* 137:1393–1401. doi:10.1083/jcb.137.6.1393

Sarker, R., M. Grønborg, B. Cha, S. Mohan, Y. Chen, A. Pandey, D. Litchfield, M. Donowitz, and X. Li. 2008. Casein kinase 2 binds to the C terminus of Na+/H+ exchanger 3 (NHE3) and stimulates NHE3 basal activity by phosphorylating a separate site in NHE3. *Mol. Biol. Cell*. 19:3859–3870. doi:10.1091/mbc.E08-01-0019

Sarno, S., H. Reddy, F. Meggio, M. Ruzzene, S.P. Davies, A. Donella-Deana, D. Shugar, and L.A. Pinna. 2001. Selectivity of 4,5,6,7-tetrabromobenzotriazole, an ATP site-directed inhibitor of protein kinase CK2 ('casein kinase-2'). *FEBS Lett.* 496:44–48. doi:10.1016/S0014-5793(01)02404-8

Schmidt, A., D.I. Utepbergenov, G. Krause, and I.E. Blasig. 2001. Use of surface plasmon resonance for real-time analysis of the interaction of ZO-1 and occludin. *Biochem. Biophys. Res. Commun.* 288:1194–1199. doi:10.1006/bbrc.2001.5914

Schmidt, A., D.I. Utepbergenov, S.L. Mueller, M. Beyermann, J. Schneider-Mergener, G. Krause, and I.E. Blasig. 2004. Occludin binds to the SH3-hinge-GuK unit of zonula occludens protein 1: potential mechanism of tight junction regulation. *Cell. Mol. Life Sci.* 61:1354–1365. doi:10.1007/s00018-004-4010-6

Schulzke, J.D., A.H. Gitter, J. Mankertz, S. Spiegel, U. Seidler, S. Amasheh, M. Saitou, S. Tsukita, and M. Fromm. 2005. Epithelial transport and barrier function in occludin-deficient mice. *Biochim. Biophys. Acta*. 1669:34–42. doi:10.1016/j.bbamem.2005.01.008

Schwark, J.R., H.W. Jansen, H.J. Lang, W. Krick, G. Burckhardt, and M. Hropot. 1998. S3226, a novel inhibitor of Na+/H+ exchanger subtype 3 in various cell types. *Pflugers Arch.* 436:797–800. doi:10.1007/s004240050704

Seth, A., P. Sheth, B.C. Elias, and R. Rao. 2007. Protein phosphatases 2A and 1 interact with occludin and negatively regulate the assembly of tight junctions in the CACO-2 cell monolayer. *J. Biol. Chem.* 282:11487–11498. doi:10.1074/jbc.M610597200

Shen, L., and J.R. Turner. 2005. Actin depolymerization disrupts tight junctions via caveolae-mediated endocytosis. *Mol. Biol. Cell*. 16:3919–3936. doi:10.1091/mbc.E04-12-1089

Shen, L., C.R. Weber, and J.R. Turner. 2008. The tight junction protein complex undergoes rapid and continuous molecular remodeling at steady state. *J. Cell Biol.* 181:683–695. doi:10.1083/jcb.200711165

Shen, L., C.R. Weber, D.R. Raleigh, D. Yu, and J.R. Turner. 2011. Tight junction pore and leak pathways: a dynamic duo. *Annu. Rev. Physiol.* 73:283–309. doi:10.1146/annurev-physiol-012110-142150

Shin, K., and B. Margolis. 2006. ZOning out tight junctions. *Cell*. 126:647–649. doi:10.1016/j.cell.2006.08.005

Siddiqui-Jain, A., D. Drygin, N. Streiner, P. Chua, F. Pierre, S.E. O'Brien, J. Bliesath, M. Omori, N. Huser, C. Ho, et al. 2010. CX-4945, an orally bioavailable selective inhibitor of protein kinase CK2, inhibits prosurvival and angiogenic signaling and exhibits antitumor efficacy. *Cancer Res.* 70:10288–10298. doi:10.1158/0008-5472.CAN-10-1893

Simon, D.B., Y. Lu, K.A. Choate, H. Velazquez, E. Al-Sabban, M. Praga, G. Casari, A. Bettinelli, G. Colussi, J. Rodriguez-Soriano, et al. 1999. Paracellin-1, a renal tight junction protein required for paracellular Mg2+ resorption. *Science*. 285:103–106. doi:10.1126/science.285.5424.103

Smales, C., M. Ellis, R. Baumber, N. Hussain, H. Desmond, and J.M. Staddon. 2003. Occludin phosphorylation: identification of an occludin kinase in brain and cell extracts as CK2. *FEBS Lett.* 545:161–166. doi:10.1016/S0014-5793(03)00525-8

Sundstrom, J.M., B.R. Tash, T. Murakami, J.M. Flanagan, M.C. Bewley, B.A. Stanley, K.B. Gonsar, and D.A. Antonetti. 2009. Identification and analysis of occludin phosphosites: a combined mass spectrometry and bioinformatics approach. *J. Proteome Res.* 8:808–817. doi:10.1021/pr7007913

Suzuki, T., B.C. Elias, A. Seth, L. Shen, J.R. Turner, F. Giorgianni, D. Desiderio, R. Guntaka, and R. Rao. 2009. PKC eta regulates occludin phosphorylation and epithelial tight junction integrity. *Proc. Natl. Acad. Sci. USA*. 106:61–66. doi:10.1073/pnas.0802741106

Tamura, A., H. Hayashi, M. Imasato, Y. Yamazaki, A. Hagiwara, M. Wada, T. Noda, M. Watanabe, Y. Suzuki, and S. Tsukita. 2011. Loss of claudin-15, but not claudin-2, causes Na(+) deficiency and glucose malabsorption in mouse small intestine. *Gastroenterology*. 140:913–923. doi:10.1053/j.gastro.2010.08.006

Tanaka, M., R. Kamata, and R. Sakai. 2005. EphA2 phosphorylates the cytoplasmic tail of Claudin-4 and mediates paracellular permeability. *J. Biol. Chem.* 280:42375–42382. doi:10.1074/jbc.M503786200

Tsukita, S., and M. Furuse. 2000. Pores in the wall: claudins constitute tight junction strands containing aqueous pores. *J. Cell Biol.* 149:13–16. doi:10.1083/jcb.149.1.13

Tsukita, S., and M. Furuse. 2002. Claudin-based barrier in simple and stratified cellular sheets. *Curr. Opin. Cell Biol.* 14:531–536. doi:10.1016/S0955-0674(02)00362-9

Turner, J.R. 2009. Intestinal mucosal barrier function in health and disease. *Nat. Rev. Immunol.* 9:799–809. doi:10.1038/nri2653

Turner, J.R., B.K. Rill, S.L. Carlson, D. Carnes, R. Kerner, R.J. Mrsny, and J.L. Madara. 1997. Physiological regulation of epithelial tight junctions is associated with myosin light-chain phosphorylation. *Am. J. Physiol.* 273:C1378–C1385.

Turner, J.R., E.D. Black, J. Ward, C.M. Tse, F.A. Uchwat, H.A. Alli, M. Donowitz, J.L. Madara, and J.M. Angle. 2000. Transepithelial resistance can be regulated by the intestinal brush-border $Na^{(+)}/H^{(+)}$ exchanger NHE3. *Am. J. Physiol. Cell Physiol.* 279:C1918–C1924.

Umeda, K., J. Ikenouchi, S. Katahira-Tayama, K. Furuse, H. Sasaki, M. Nakayama, T. Matsui, S. Tsukita, M. Furuse, and S. Tsukita. 2006. ZO-1 and ZO-2 independently determine where claudins are polymerized in tight-junction strand formation. *Cell*. 126:741–754. doi:10.1016/j.cell.2006.06.043

Van Itallie, C., C. Rahner, and J.M. Anderson. 2001. Regulated expression of claudin-4 decreases paracellular conductance through a selective decrease in sodium permeability. *J. Clin. Invest.* 107:1319–1327. doi:10.1172/JCI12464

Van Itallie, C.M., A.S. Fanning, and J.M. Anderson. 2003. Reversal of charge selectivity in cation or anion-selective epithelial lines by expression of different claudins. *Am. J. Physiol. Renal Physiol.* 285:F1078–F1084.

Van Itallie, C.M., O.R. Colegio, and J.M. Anderson. 2004. The cytoplasmic tails of claudins can influence tight junction barrier properties through effects on protein stability. *J. Membr. Biol.* 199:29–38. doi:10.1007/s00232-004-0673-z

Van Itallie, C.M., T.M. Gambling, J.L. Carson, and J.M. Anderson. 2005. Palmitoylation of claudins is required for efficient tight-junction localization. *J. Cell Sci.* 118:1427–1436. doi:10.1242/jcs.01735

Van Itallie, C.M., L. Betts, J.G. Smedley III, B.A. McClane, and J.M. Anderson. 2008a. Structure of the claudin-binding domain of Clostridium perfringens enterotoxin. *J. Biol. Chem.* 283:268–274. doi:10.1074/jbc.M708066200

Van Itallie, C.M., J. Holmes, A. Bridges, J.L. Gookin, M.R. Coccaro, W. Proctor, O.R. Colegio, and J.M. Anderson. 2008b. The density of small tight junction pores varies among cell types and is increased by expression of claudin-2. *J. Cell Sci.* 121:298–305. doi:10.1242/jcs.021485

Van Itallie, C.M., A.S. Fanning, A. Bridges, and J.M. Anderson. 2009a. ZO-1 stabilizes the tight junction solute barrier through coupling to the perijunctional cytoskeleton. *Mol. Biol. Cell*. 20:3930–3940. doi:10.1091/mbc.E09-04-0320

Van Itallie, C.M., J. Holmes, A. Bridges, and J.M. Anderson. 2009b. Claudin-2-dependent changes in noncharged solute flux are mediated by the extracellular domains and require attachment to the PDZ-scaffold. *Ann. N. Y. Acad. Sci.* 1165:82–87. doi:10.1111/j.1749-6632.2009.04052.x

Van Itallie, C.M., A.S. Fanning, J. Holmes, and J.M. Anderson. 2010. Occludin is required for cytokine-induced regulation of tight junction barriers. *J. Cell Sci.* 123:2844–2852. doi:10.1242/jcs.065581

Walter, J.K., V. Castro, M. Voss, K. Gast, C. Rueckert, J. Piontek, and I.E. Blasig. 2009. Redox-sensitivity of the dimerization of occludin. *Cell. Mol. Life Sci.* 66:3655–3662. doi:10.1007/s00018-009-0150-z

Wang, F., W.V. Graham, Y. Wang, E.D. Witkowski, B.T. Schwarz, and J.R. Turner. 2005. Interferon-gamma and tumor necrosis factor-alpha synergize to induce intestinal epithelial barrier dysfunction by up-regulating myosin light chain kinase expression. *Am. J. Pathol.* 166:409–419. doi:10.1016/S0002-9440(10)62264-X

Weber, C.R., S.C. Nalle, M. Tretiakova, D.T. Rubin, and J.R. Turner. 2008. Claudin-1 and claudin-2 expression is elevated in inflammatory bowel disease and may contribute to early neoplastic transformation. *Lab. Invest.* 88:1110–1120. doi:10.1038/labinvest.2008.78

Weber, C.R., D.R. Raleigh, L. Su, L. Shen, E.A. Sullivan, Y. Wang, and J.R. Turner. 2010. Epithelial myosin light chain kinase activation induces mucosal interleukin-13 expression to alter tight junction ion selectivity. *J. Biol. Chem.* 285:12037–12046. doi:10.1074/jbc.M109.064808

Wittchen, E.S., J. Haskins, and B.R. Stevenson. 1999. Protein interactions at the tight junction. Actin has multiple binding partners, and ZO-1 forms independent complexes with ZO-2 and ZO-3. *J. Biol. Chem.* 274:35179–35185. doi:10.1074/jbc.274.49.35179

Wong, V. 1997. Phosphorylation of occludin correlates with occludin localization and function at the tight junction. *Am. J. Physiol.* 273:C1859–C1867.

Yu, A.S., K.M. McCarthy, S.A. Francis, J.M. McCormack, J. Lai, R.A. Rogers, R.D. Lynch, and E.E. Schneeberger. 2005. Knockdown of occludin expression leads to diverse phenotypic alterations in epithelial cells. *Am. J. Physiol. Cell Physiol.* 288:C1231–C1241. doi:10.1152/ajpcell.00581.2004

Yu, A.S., M.H. Cheng, S. Angelow, D. Günzel, S.A. Kanzawa, E.E. Schneeberger, M. Fromm, and R.D. Coalson. 2009. Molecular basis for cation selectivity in claudin-2-based paracellular pores: identification of an electrostatic interaction site. *J. Gen. Physiol.* 133:111–127. doi:10.1085/jgp.200810154

Yu, D., A.M. Marchiando, C.R. Weber, D.R. Raleigh, Y. Wang, L. Shen, and J.R. Turner. 2010. MLCK-dependent exchange and actin binding region-dependent anchoring of ZO-1 regulate tight junction barrier function. *Proc. Natl. Acad. Sci. USA*. 107:8237–8241. doi:10.1073/pnas.0908869107

Zeissig, S., N. Bürgel, D. Günzel, J. Richter, J. Mankertz, U. Wahnschaffe, A.J. Kroesen, M. Zeitz, M. Fromm, and J.D. Schulzke. 2007. Changes in expression and distribution of claudin 2, 5 and 8 lead to discontinuous tight junctions and barrier dysfunction in active Crohn's disease. *Gut*. 56:61–72. doi:10.1136/gut.2006.094375

Zolotarevsky, Y., G. Hecht, A. Koutsouris, D.E. Gonzalez, C. Quan, J. Tom, R.J. Mrsny, and J.R. Turner. 2002. A membrane-permeant peptide that inhibits MLC kinase restores barrier function in in vitro models of intestinal disease. *Gastroenterology*. 123:163–172. doi:10.1053/gast.2002.34235

Published May 2, 2011

Raleigh et al., http://www.jcb.org/cgi/content/full/jcb.201010065/DC1

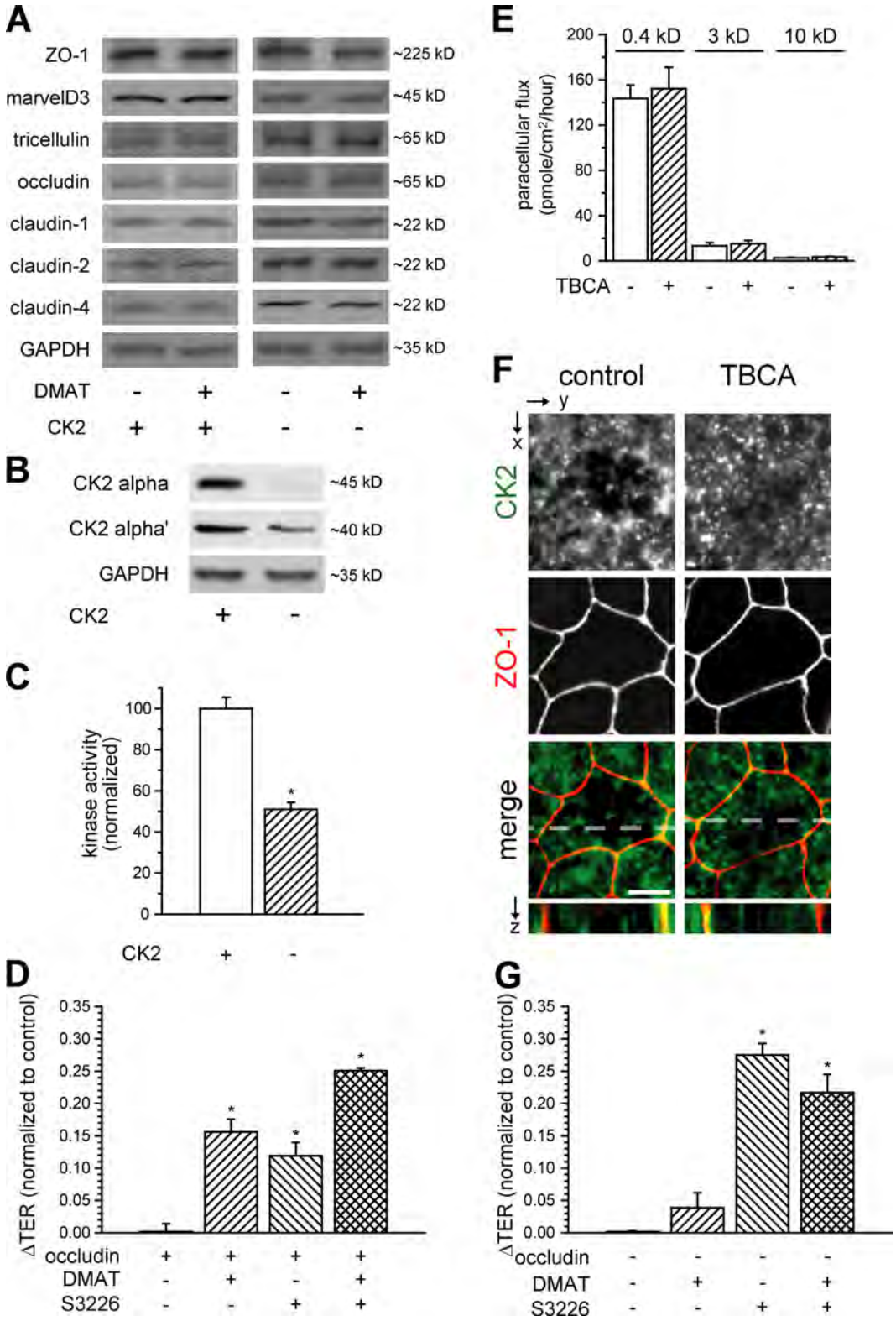

Published May 2, 2011

Figure S1. **Contributions of CK2 to barrier regulation.** (A) SDS-PAGE immunoblot analysis of Caco-2 monolayers demonstrated equivalent TJ protein expression after either 50 μM DMAT or combined CK2α/α′ knockdown. Data are representative of four experiments. (B) Caco-2 cells treated with either control, or combined CK2α- and CK2α′-targeting siRNAs; protein suppression was assessed by SDS-PAGE immunoblot. These analyses revealed 89 ± 5% and 58 ± 8% reductions in CK2α and CK2α′ protein expression, respectively. Data are representative of four experiments, each in triplicate. (C) CK2 knockdown markedly reduced CK2 kinase activity in Caco-2 monolayers. Data are representative of ≥2 experiments, each in duplicate. (D) CK2 inhibition (50 μM DMAT) elevated TER by 16 ± 2%. NHE3 inhibition with 50 μM S3226 produced a comparable increase in barrier function (12 ± 2%). Combined CK2 and NHE3 inhibition had an additive effective on barrier function and raised TER by 25 ± 1%. TER data were normalized to vehicle control treatment, are shown after 4 h of treatment, and are representative of two experiments, each in triplicate. (E) 50 μM TBCA treatment failed to alter the flux of free FITC (MW 389 D), 3 kD FITC-dextran, or 10 kD FITC-dextran conjugates across Caco-2 monolayers. Data represent the average of two experiments, each with $n = 4$. (F) Immunofluorescence microscopy demonstrates overlap of CK2 (green) and ZO-1 (red) fluorescence at the TJ, as well as CK2-associated fluorescence along lateral membranes and within the cytoplasm. 50 μM TBCA failed to redistribute CK2. Bar, 10 μM. Images are representative of three experiments, each in duplicate. (G) Occludin knockdown in Caco-2 monolayers eliminated TER response to CK2 inhibition (4 ± 2%) without attenuating NHE3-mediated barrier regulation (27 ± 1% alone; 22 ± 3% in combination with DMAT). TER data were normalized to vehicle control treatment (163 ± 4 Ohms × cm^2), are shown after 4 h of treatment, and are representative of two experiments, each in triplicate.

Published May 2, 2011

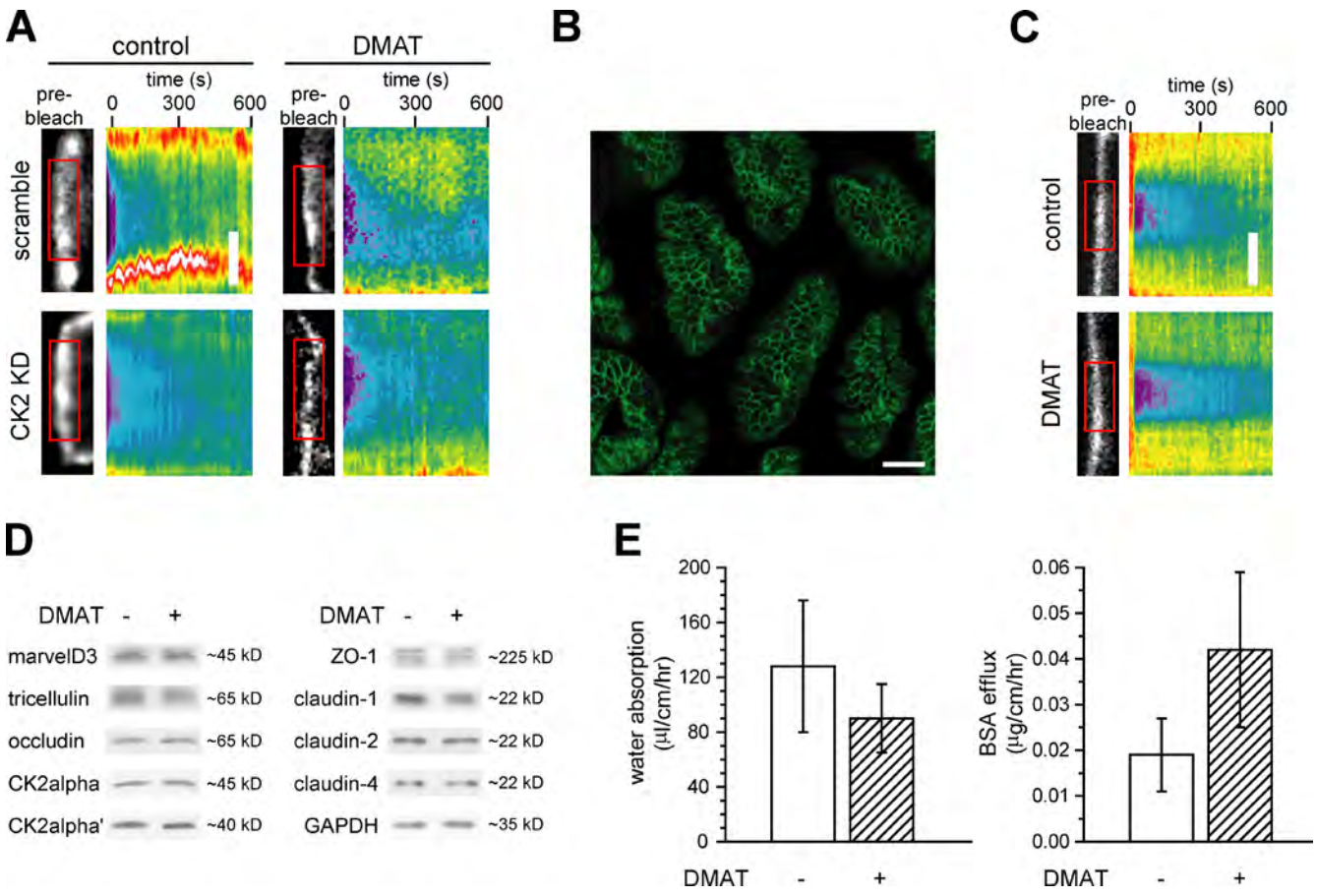

Figure S2. **Contributions of CK2 to in vitro and in vivo occludin exchange as well as in vivo transport and barrier function.** (A) Kymographs indicate that CK2 knockdown in Caco-2 monolayers with CK2α- and CK2α′-targeted siRNAs (CK2 KD) reduces the mobile fraction of EGFP-occludin to an extent comparable to 50 µM DMAT and also renders occludin exchange insensitive to CK2 inhibitors. Kymographs are representative of ≥4 experiments. (B) Low magnification image of jejunal villi in EGFP-occludin transgenic mice. Bar, 50 µm. (C) Kymographs show that CK2 inhibition (50 µM DMAT) decreases the mobile fraction of EGFP-occludin at the TJ in vivo. In vivo FRAP data are representative of ≥40 bleached regions from each of two mice for each condition. (D) SDS-PAGE analysis of wild-type mouse jejunal enterocytes revealed equivalent expression of TJ proteins and the catalytic subunits of CK2 after perfusion of 50 µM DMAT or vehicle. SDS-PAGE immunoblot data are representative of two experiments, each in duplicate. (E) Water absorption and BSA efflux were comparable across mouse jejunum after perfusion with either vehicle or 50 µM DMAT. Data represent two mice for each condition.

Published May 2, 2011

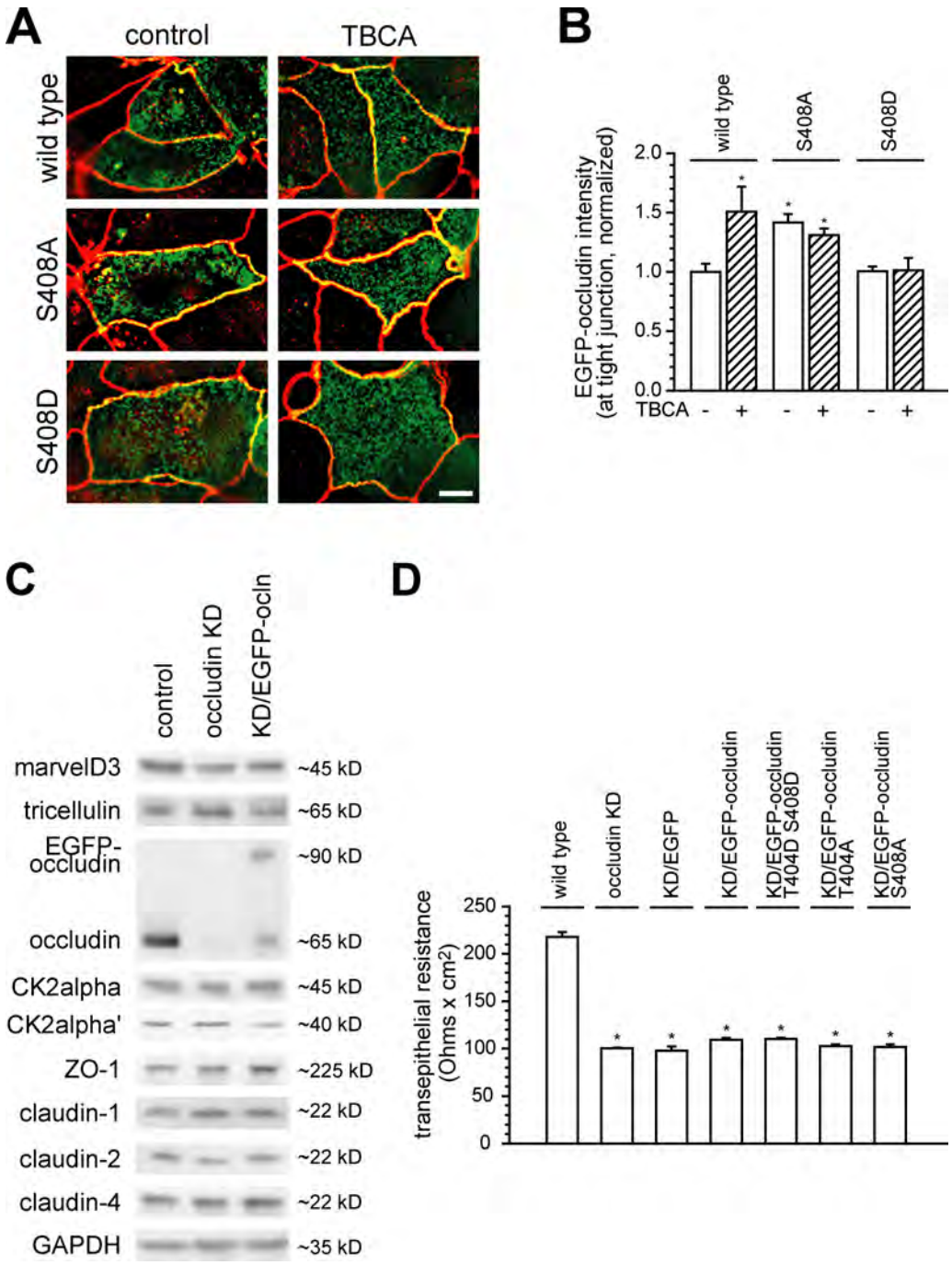

Figure S3. **Subcellular distribution and functional impact of occludin mutants.** (A) Examination of EGFP-occludin (green) and ZO-1 (red) localizations in Caco-2 monolayers demonstrated redistribution of wild-type EGFP-occludin in response to CK2 inhibition (50 µM TBCA). EGFP-occludin S408A was enriched at the TJ in the absence of CK2 inhibition, relative to wild-type and S408D EGFP-occludin, and neither mutant was redistributed in response to 50 µM TBCA. Bar, 10 µm. Data are representative of two independent experiments. (B) Morphometric analysis shows enrichment of wild-type EGFP-occludin at the TJ after CK2 inhibition, enrichment of S408A occludin at the TJ at steady state, and no change in the localization of either S408A or S408D EGFP-occludin after CK2 inhibition. Data from matched exposures of monolayers treated with either 50 µM TBCA or vehicle were calculated using ≥6 cells per condition and are representative of two experiments. (C) SDS-PAGE immunoblot analysis of wild-type, occludin knockdown, and occludin knockdown/EGFP-occludin (KD/EGFP-occludin) cell lines. EGFP-occludin expression in occludin knockdown lines was at lower levels than endogenous occludin (in control Caco-2). Expression of other TJ proteins was unaffected by occludin expression or knockdown, as was CK2 expression. Data are representative of two experiments, each in quadruplicate. (B) Occludin knockdown cell lines demonstrated significantly lower TER than wild-type Caco-2 monolayers ($P < 0.05$). Expression of free EGFP, wild-type, and mutant EGFP-occludin proteins in occludin knockdown cell lines failed to restore TER. Data are representative of ≥3 stable cell lines for each construct, each assayed in triplicate.

Published May 2, 2011

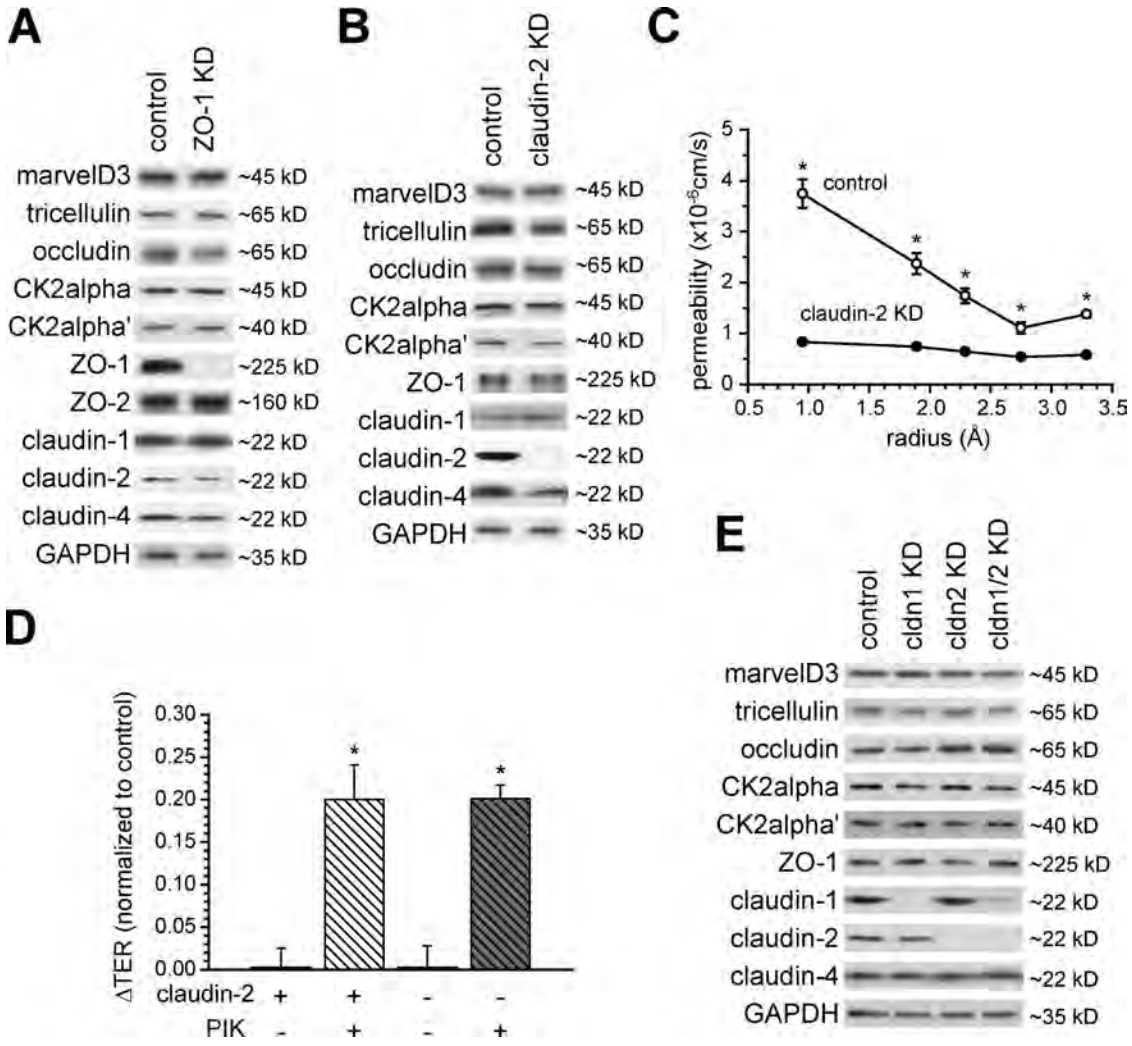

Figure S4. **Analyses of ZO-1, claudin-1, and claudin-2 knockdown Caco-2 cells.** (A) SDS-PAGE immunoblot of ZO-1 knockdown and control Caco-2 cell lines demonstrated >90% suppression of ZO-1 expression. ZO-2, CK2, claudin-1, claudin-4, occludin, tricellulin, and marvelD3 expression were equivalent in ZO-1 knockdown and control monolayers. There was, however, a minor reduction in claudin-2 protein expression in ZO-1 knockdown monolayers. (B) SDS-PAGE immunoblot of claudin-2 knockdown and control Caco-2 cell lines demonstrated >90% suppression of claudin-2 expression. Expression of other TJ proteins and CK2 was unaffected. Data are representative of three experiments, each in duplicate. (C) Claudin-2 knockdown reduced paracellular flux of small and larger cations. Data are representative of two experiments, each with $n = 4$. (D) MLCK inhibition (250 μM PIK) increased TER of claudin-2 knockdown and control monolayers comparably. TER data were normalized to vehicle control treatment for control (239 ± 11 Ohms × cm^2) and claudin-2 knockdown cell lines (1173 ± 51 Ohms × cm^2), and are representative of ≥3 experiments, each in triplicate. (E) SDS-PAGE immunoblot of Caco-2 monolayers after transient claudin-1 knockdown, stable claudin-2 knockdown, or both demonstrated >90% suppression of claudin expression. Expression of CK2, ZO-1, claudin-2, claudin-4, occludin, tricellulin, and marvelD3 was equivalent between knockdown and control monolayers; data are representative of two experiments, each in triplicate.